Mapping of Material & Conversion Parameters of Packaging Production – Boardio®

by

Younes Chraibi Ottosson
&
Yusuf Qasem

Master Thesis Number: 2022-06

Department of Chemical Engineering
Lund University
&
Graphic Packaging International, Inc.

June 2022

Supervisor (LTH): **Professor Bernt Nilsson**
Co-supervisor (GPI): **Technical Manager Max Hallin**
Examiner (LTH): **Professor Christian Hulteberg**

Postal address	**Visiting address**	**Telephone**
Box 124	Kemicentrum	+46 46-222 82 85
SE-221 00 Lund, Sweden	Naturvetarvägen 14	+46 46-222 00 00
Web address	223 62 Lund, Sweden	
http://www.lth.se/chemeng/		

Preface

The work described in this master thesis was performed at Graphic Packaging International Inc. (GPI), Lund 2022. We wish to thank all involved parts at GPI, especially to Plant Director Rosemary Pålsson and Technical Manager/Supervisor Max Hallin for giving us this opportunity and believing in us. A warm thanks to the production leaders along with the quality, engineering, and supply-chain departments for enabling this work and supporting us along the way. Further, we would like to thank all machine operators involved along the extrusion lamination, sheeting and die-cutting, you are the cornerstone of the company.

We would also like to thank our supervisor Professor Bernt Nilsson and examiner Professor Christian Hulteberg at the Department of Chemical Engineering, LTH, for your support and guidance during this master thesis. A big thanks to Research Engineer Jonas Engqvist at the Department of Solid Mechanics, LTH, for facilitating the data acquisition and measurements carried out in the 3D x-ray microscope at the 4D Imaging Lab of our paperboard laminates. The level of detail and information presented in the 3D projections were crucial for strengthening the conclusions of this master thesis.

To our families and closest relatives, we would like to show our gratitude and thankfulness for your never-ending support when needed. Finally, we would like to thank our mothers Khawla Zainal Abdeen and Lisbeth Ottosson, for bringing us to this world and for all the sacrifices you have made for us.

"I have no idols. I admire work, dedication, and competence."

- Ayrton Senna, 1960-1994

Abstract

With an increased demand for sustainable packaging solutions for the ever-growing FMCG market, fiber-based systems rise as an answer to phasing out plastics in packages and reducing the humanity's climate footprint. However, constructing a packaging solution largely consisting of paperboard comes with its challenges, such as integrating functionalities in the anisotropic paperboard that formerly were provided by a fundamentally different materials with divergent mechanical properties, being isotropic polymers. In the pursuit of a fiber-based packaging system, Boardio® was created.

Three different commercial paperboards with different mechanical properties together with three different laminate structures, creating nine paperboard laminates in total, were studied. The main objective of this thesis was to investigate how different laminate structures, together with machine parameters affect the crease height and strength of the perforations in the Boardio® solution. The work was centred around quantitative analysis through tensile strength testing of laminate substrates and thickness measurements of paperboard laminate creases, together with separate qualitative analyses through optic microscopy and x-ray tomography.

Opposed to the ideal theoretical behaviour and mechanics of paperboard laminates and perforations which gain strength when adding more components such as PE-film and aluminium foil to the laminate, it was found that thicker laminates yield in lower, but less fluctuating, perforation strengths than laminates without PE-film and aluminium foil. The lower strength is related to the higher degree of rupture in the paperboard of the perforations, validated with x-ray tomography. Through this qualitative method of validation, it was possible to identify a total rupture in the paperboard of full laminates, being laminates with the structure paperboard/PE /al-foil/PE/PE-film, most plausibly caused during the formation of creases in the die-cutting process, which induces large stresses in the paperboard laminate. This additionally strengthened the importance of including a layer of PE-film to obtain satisfying, non-fluctuating, perforation strength. Further, the strength of the perforations is strictly governed by the degree on non-ruptured fibers in laminates without PE-film, making it challenging to reach non fluctuating perforation strength during large volume productions of these laminates. It was also found that thicker laminates yield in deeper creases during the die-cutting process, enabling better folding, and finishing of the Boardio® packages.

Sammanfattning

Med en ökad efterfrågan på hållbara förpackningslösningar för den ständigt växande FMCG-marknaden, uppenbarar sig fiberbaserade system som ett svar på att fasa ut plast i förpackningar och minska vårt klimatavtryck. Att konstruera en förpackningslösning som till stor del består av kartong kommer med sina utmaningar, som att integrera funktioner i kartongen som polymerer tidigare bidragit till. Då polymerer i förpackningar är isotropa och har starkt divergerande egenskaper från anisotropiskt papper, ställer detta helt nya krav på förpackningstillverkningen. I jakten på ett fiberbaserat förpackningssystem skapades Boardio®.

Tre olika kommersiella kartonger med olika mekaniska egenskaper tillsammans med tre olika laminatstrukturer, vilket skapar totalt nio kartonglaminat, studerades i detta examensarbete. Huvudsyftet med detta examensarbete var att undersöka hur olika laminatstrukturer, tillsammans med maskinparametrar, påverkar bighöjden och styrkan hos perforeringen i Boardio® förpackningen. Arbetet var centrerat kring kvantitativ analys genom draghållfasthetstestning av laminatsubstrat och tjockleksmätningar av bighöjden i laminaten, tillsammans med separata kvalitativa analyser genom optisk mikroskopi och röntgentomografi.

I motsats till det ideala teoretiska beteendet och mekaniken hos kartonglaminat och perforeringar som ökar i styrka när man lägger till fler komponenter som PE-film och aluminiumfolie till laminatet, visades att tjockare laminat ger lägre, men mindre fluktuerande, perforeringsstyrkor än laminat utan PE-film och aluminiumfolie. Den lägre hållfastheten är relaterad till den högre graden av ruptur i kartongen, vilket validerades med röntgentomografi. Genom denna kvalitativa valideringsmetod var det möjligt att identifiera en fullständig ruptur i kartongen för alla laminat med samtliga komponenter, vilket är laminat med strukturen kartong/PE/al-folie/PE/PE-film. Rupturen orsakades högst troligen av påfrestningarna i laminatet som skapas under bigning i stansprocessen. Detta stärkte ytterligare vikten av att inkludera ett lager av PE-film för att erhålla tillfredsställande, icke-fluktuerande, öppningskrafter i perforeringen. Vidare visades även att hållfastheten hos perforeringarna i laminat utan PE-film strikt styrs av graden icke förstörda fiber i perforeringarna, vilket gör det betydligt mycket mer utmanande att uppnå icke fluktuerande öppningskrafter under produktion av stora volymer med dessa laminat. Det visade sig också att tjockare laminat i stansningsprocessen ger djupare bigar, vilket möjliggör bättre vikning och efterbehandling av Boardio® förpackningarna.

Table of Contents

1 Introduction

As a result of an increased demand from society demanding a packaging system with less plastic content that is more sustainable, Boardio® was launched by Graphic Packaging International Systems, formerly known as AR Packaging Systems. The purpose of this launch was to develop a packaging system that challenges old conventional packaging technologies, functionalities, materials, and features along with their reliability on plastic parts, while at the same time promising great efficiency and adaptability. Boardio® stands out clearly from its predecessor, being Cekacan® & Sealio®, and competing systems, as it does not contain any injection-molded plastic parts while at the same time being able to provide the same functionalities and features.

During 2021 AR Packaging Systems AB with headquarters in Lund was acquired by Graphic Packaging International (GPI) inc. AR Packaging itself is a Swedish packaging company with a history reaching back to the year 1929. The Systems-division of the company develops and manufactures packaging material and packaging machine systems mainly aimed for dry food products. All production and development takes place in Lund, while products and machine systems are sold and distributed within the borders of Europe, North America, and Asia. [1]

Produced packages consists of paperboard and polymer laminates which in turn constitutes the packaging systems Cekacan®, Sealio®, Hermetet® and Boardio®. The latter, being the Boardio® system, is the most recently launched packaging system and the system that this master thesis will revolve around. The Boardio-system puts new and certain demands on the packaging material, the converting process, and the package itself that differs from the demands from the rest of the systems. [1]

1.1 Project Description

At the time of this project, Boardio® was still considered a new product and the commercial production had just recently started to scale up towards volumes of the older systems. This further implies that some stages of the production process of the system still is in the development phase. Previous functionalities of the injection molded plastic lid in the Cekacan® and Sealio® system is integrated into the laminate body of the Boardio® system, which in turn puts more demands on the material since the functionality of the package now relies solely on the properties of the laminate.

Five components make up the Boardio® package and these are: the top lid, opening membrane, body, tape, and base, as depicted in Figure 1. All the components, except for the tape, are produced in Lund by extrusion, lamination, sheeting, printing and ultimately die-cutting. A Boardio® body consists of curl creases at the top and the bottom (and in some cases vertically across the body) that enables the material to curl around the top lid, opening membrane, and base. When set side by side with the other systems, the opening mechanism of Boardio® constitutes of perforations in close proximity to the top curl creases, instead of an injection molded plastic lid.

Figure 1. Depicts the five components that makes up the Boardio® package along with a final assembled package. (Courtesy of: Graphic Packaging International)

There are demands on both the curl creases and perforation. The larger the depth is of the curl creases the better it gets curled around top lid and base, while a shallow curl crease could possibly result in crashes of the package in the Boardio® line. In addition, the perforations must be strong enough to hold the package together during production and transportation but cannot be too strong leading to a package that is hard to open or opens incorrectly.

1.2 Aim & Scope

The aim of this master thesis is to investigate, understand and map the parameters in the varied materials and production steps of the components in the Boardio® system. This study will not investigate or include the printing process as this step is known for not affecting the mechanic material properties of the laminates. Ultimately, the aim is to provide an answer to the question: which materials are deemed suitable for the Boardio® system with respect to producibility and openability, and which are not suitable? The focus will be towards the body component of the system, as it is the most crucial component with regards to the functionalities mentioned earlier.

The answers will be based on quantitative analysis of the crease height and the opening force of the perforations of samples produced in a flatbed die-cutter along with some other production methods. As an aid and validation to the quantitative analysis, a qualitative analysis will be conducted utilizing both an optical microscope and x-ray computed tomography.

It is worth mentioning that this report will not go into thorough detail about the technical specifications of the different machines, procedures or materials that are to be studied due to reasons related to corporate secrecy.

1.3 Constraints

In order to narrow down and establish a reasonable project frame with respect to the time and resources given, the following constraints were set:

- Only focus on material measurements, i.e., no attempts were made on optimizing and looking at alternative components for the laminates.
- Only investigate Boardio ® body blanks, i.e., no measurements or investigations were conducted on the base, toplid or opening membrane.
- No individual tuning of die-cutter settings for each material.
- Only investigate nine materials (laminates)
- Only investigate one flatbed die-cutter configuration.

2 Background & Theory

Before introducing the challenge at hand, it can be useful to gain a deeper insight in the general production process at Graphic Packaging International Systems (abbreviated GPI), together with general knowledge about the system and paperboard properties. This section aims to introduce the production process and to identify the challenges that are to be studied in this thesis. The fundamentals of paper and paperboard material properties as well as their production processes will also be discussed, as the studied laminates are made up of a majority of paperboard. Consequently, the paperboard has a considerable influence on the properties of the final package.

2.1 General Description of Package Production Process at GPI

This study was based on and done in accordance with the production site of GPI located in Lund. In short, the production process of packages can be described in the following chronological order: lamination, sheeting, printing, die-cutting and folding into final product, as depicted in Figure 2. The production process begins with receival of material from different suppliers. After which the materials that are in question for a certain package are combined in the lamination process.

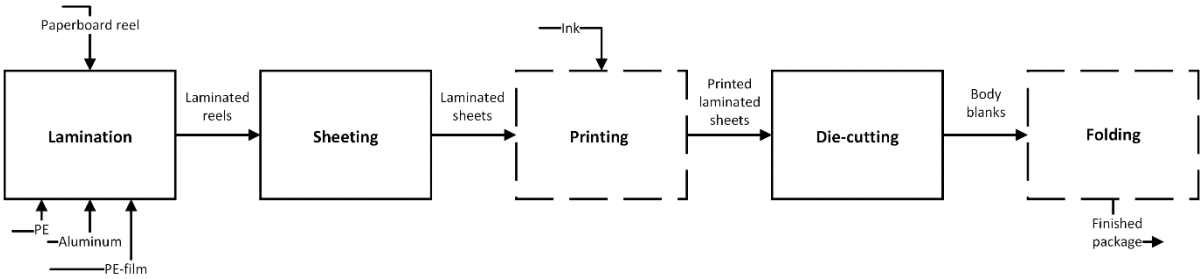

Figure 2. Depicts an overview of the packaging production process at GPI. Process steps illustrated with dashed lines are process steps that are not within the scope of this study.

The purpose of the lamination process is to enhance the functional usage of paperboard by combining several layers of different materials through extrusion. In the extrusion lamination, paperboard is coated with different layers consisting of, aluminum (al-foil), polyethylene (PE) and PE-film. Depending on the desired material composition of the final laminate, the materials are combined in different orders and thickness. Lamination can be done in several separate ways that are differentiated by the adhesive system used for each lamination process. These include: lamination with water-based adhesives (wet-bond lamination), dry-bond lamination, wax lamination and ultimately extrusion lamination. [2] The latter is the system used at GPI's site in Lund.

In the extrusion lamination the paperboard reels are unwound, and molten PE is extruded onto the paperboard. Extrusion of molten PE enables the lamination of aluminum foil onto the paperboard. PE acts as an adhesive agent in this case. The now laminated paperboard can go two ways, either it is laminated with a PE blend once again in order to ease the lamination of another film layer or wound into a reel once again. After the lamination, the material is cut into a web width of choice and then wound up to a reel for further processing.

Following the extrusion lamination process is the sheeting, where the laminate reel is cut into sheets with adequate lengths before being collected in a pile on a pallet. The cut-off length greatly depends on the requirements of the printing machine and the die-cutting format. Compared to the other process steps of producing laminate packaging, the sheeting process is less complex when compared to the extrusion-lamination process. The main requirement of produced sheets is to minimize curl, describing the bending of the material in either laminate or paperboard direction. High curl in either direction causes production disturbance in the printing- and die-cutting processes. The de-curling is done by adjusting the force applied by the rolls as the web passes through the machine. The limiting factor of how much a laminate can be de-curled is the formation of cracks in the paperboard, and the tendency for cracks to form depends on the paperboard-type and paper fiber structure, the storage time between extrusion lamination, the relative humidity, and the laminate structure [3]. The sheeting is proceeded by the printing in which the sheets are printed with the graphical profile of the container which differs depending on the customer.

Die-cutting is the production step in the converting process of paperboard that includes creasing and cutting of printed sheets into body blanks [4, 5]. Cutting and creasing can be done using either a flatbed or a rotary die, with the difference being that cutting is done while the paperboard is stationary in the flatbed die-cutter, and in the rotary die-cutter, the board is moving [5]. Flatbed die-cutting is normally sheet fed while rotary die-cutting usually is reel-fed, both of which are operated following the printing stage. In the case of GPI, both a sheet fed rotary die-cutting machine and a sheet fed flatbed die-cutting machine is used. The formation of creases and perforation occurs simultaneously in the cutting section at the flatbed machine, whilst they occur after one another in the rotary die-cutting machine. After the cutting section, the body blanks are separated from the rest of the sheet, being the scrap material, in the blanking section. The body blanks are then delivered onto a pallet of finished goods, hence while the scrap material is collected separately for recycling. In Figure 3, a finished Boardio® body blank can be seen. Two critical parameters must be supervised in the body blank, being the thickness of the creases and the strength of the perforation. The thickness of the creases is crucial to be of sufficient depth, since too shallow creases tend to cause unwanted plastic deformation in the material and crack formation in a later processing stage. Regarding the opening force, a too high opening force causes the package to be difficult or unable to open. Meanwhile, a too weak opening force will most likely cause the package to burst and open during shipping or handling when its intention is to be closed. These parameters are validated, and quality assured by measuring the crease height with a thickness measurement device and observing the maximum opening force of the perforation with a tensile strength testing system.

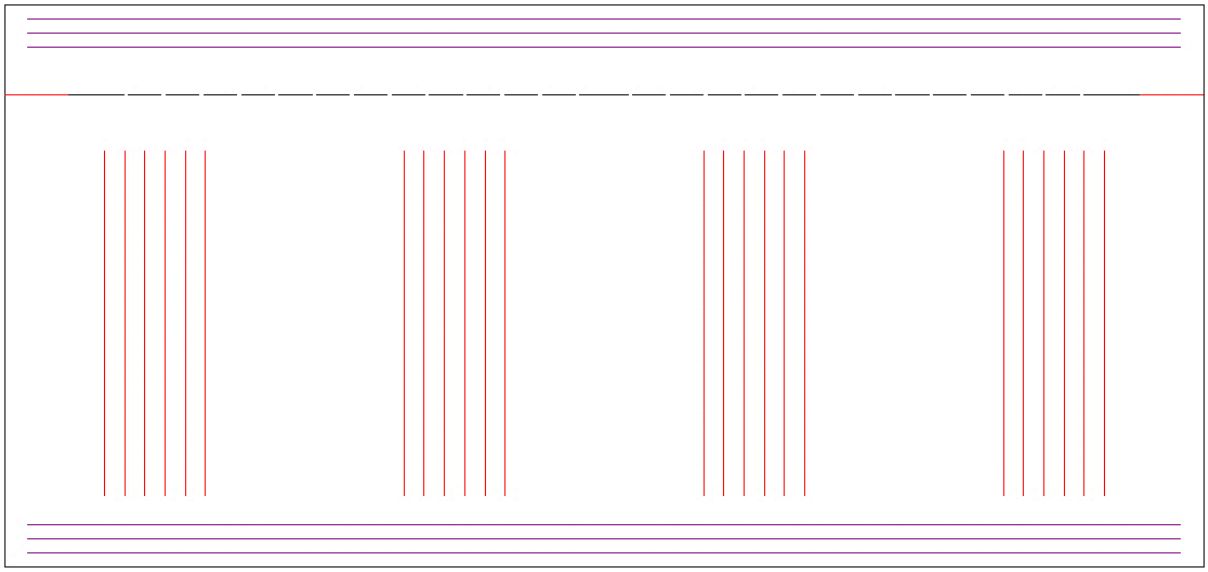

Figure 3. Depicts a finished body blank after passing the die-cutter. The creases are marked with solid lines and the perforation is marked with dashed lines.

Creasing of paperboard is done to increase the convertibility and further facilitate the folding process, which proceeds the die-cutting, as depicted in Figure 2. Without the creasing lines formed in die-cutting, the blank will not allow accurate and easy folding while at the same time not cracking in comparison to a blank with creasing lines [5]. Creasing causes delamination in between the plies of the paperboard which further reduces the bending stiffness and thus facilitates folding [6].

2.1.1 Where the Problem Arises

The main challenge at hand is to continuously produce material of invariable quality with regards to perforation strength and crease height, on all different laminates with different blank configurations, with as low set-up time and run waste as possible. Dies are constructed on site and differ depending on the structure of the laminate. One standard configuration of dies does simply not exist, and this creates a dispute with regards to reproducibility between different orders during commercial production. Dies are adjusted during operations and between jobs by altering the spacing rubber between the knifes together with applying layers of special purpose tape. The knifes in place can also be altered to different thickness, height, and sharpness, which adds another set of dimensions to the already complex problem of finding a standard procedure for flatbed die-cutting operations. The machine can also be set to different die pressures. Moreover, the singularly largest challenge lies in the relative position of the perforation and the top creases. Since the distance between the creases and the perforation is very low and the creases are formed simultaneously as the perforation (flatbed die-cutting), the creasing tends to affect the nicks (weakening the nicks) due to the induced stresses in the paperboard laminate due to the elongation in the laminate as the creases are formed. [7]

To further improve and standardize the die-cutting procedure, one must investigate with respect to the materials produced and evaluate eventual tendencies between different materials. A comprehensive understanding on how each and every commercial board behaves together with different laminate structures is necessary to minimize run-waste and set-up time. In order to do so, a material study was conducted which is described in *Materials & Methods*.

2.2 Paper and Paperboard

Paper and paperboard consist of cellulose fibers that has formed a network of bonded fibers. In order to produce and obtain this network of cellulose fibers a fibrous material is required; this can be wood, sugar canes, linen and also recycled paper. Normally, wood is used as the cellulosic fiber source, these are called virgin fibers. However, in order to obtain the cellulosic fibers, the fiber source must go through a pulping process with the aim of separating the cellulose from other fibers such as lignin and hemicellulose. [8, 9]

The terms “paper” and “paperboard” can sometimes be confusing; therefore, the International Standards Organization (ISO) has decided to separate them. According to the ISO definition, paper has a grammage of less than 250 g/m^2 and is often used in corrugated cardboard manufacture as well as sack and bag manufacture. Paperboard, on the other hand has a grammage over 250 g/m^2 and is mainly used in cartons often as laminates. [8]

2.2.1 Pulping, Bleaching Processes and Manufacture of Paperboard

The pulping process can be done with two different methods: chemical or mechanical, both of which start with wood chips as the feedstock. The main difference between the two pulping processes is that in mechanical pulping the debarked wood chips are mechanically grinded in order to obtain virgin fibers. This process results in fibers that are shorter in length which consequently yields paper of lower strength and that is considered low grade. In chemical pulping the fibers are obtained by washing and cooking the wood chips in either an alkaline (“Kraft process” or “Sulphate Process”) or acidic solution (“Sulfite process”). Although the chemical pulping processes are more expensive and energy demanding, they result in paper that is stronger and whiter. [8, 10]

Mechanical pulp can be thermo-mechanical (TMP) or chemical thermo-mechanical (CTMP). TMP process utilizes hot water to soften fibers resulting in less damaged fibers and consequently paper with higher strength in comparison to normal mechanical pulping. CTMP also utilizes hot water just like the TMP process, however with the addition of small amounts of chemicals with the aim of digesting the wood mass and removing impurities prior to pulping. Mechanical pulp is often mixed with chemical pulp to reduce costs but also to obtain desired material and strength properties of the end product. [8]

Bleaching is treatment of the fibers that proceeds the pulping process, in which the pulp is treated with bleaching agents in order to increase its brightness. Nowadays, the bleaching agent used in the process is normally hydrogen peroxide as the more traditional chlorine containing bleaching agents poses a higher safety hazard and an environmental disadvantage. What causes the bleaching of the pulp once it is mixed with the bleaching agent is the removal of lignin. This in turn gives a better fiber-to-fiber strength while at the same time reducing the length of the fibers and ultimately resulting in weaker fibers. This further means that the more extensively the pulp is bleached, the weaker the fibers become. [8, 11]

The bleaching is followed by the addition of additives in order to give the paperboard its desired properties and to aid the manufacturing process of paperboard. Examples of types of additives include fillers, pigment, whitening agents, binders, anti-foaming agents, and flocculating agents. Following the addition of additives, the fibers and additives are suspended in water and ready for the manufacture of paperboard. The manufacture of paperboard consists broadly of three stages. In which the first stage is the preparation of dilute suspension of fibers and additives in water. Followed by forming the dilute suspension into a sheet of intertwined

fibers and ultimately removal of water in all stages by drainage, pressure, and evaporation. [8, 12]

As it has been mentioned briefly up until this point, the material properties of paperboards depend on several factors. Earlier on it was mentioned that the pulping process chosen, and the grade of bleaching influences both the strength and the visual characteristics of the material. In addition to these two, factors such as source and type of fiber, extraction method of fibers, and number of plies that is used to make up the paperboard also affect the properties of the final product. All of which can be tailored in order to meet the demands of the packaging industry. [8]

2.2.2 Properties of Paperboard

The most important properties of paperboard that are to be used for packaging material are stiffness, printing surface, water absorption, burst strength, tensile strength, grease resistance, tear resistance, and compression strength. A majority of the material properties can be adjusted by combining different amounts of mechanical and chemical pulp in order to achieve desired properties. In general, the following can be concluded about the material properties of paperboard [8]:

- Increasing the amount of mechanical pulp leads to an increased stiffness of the paperboard
- An increased amount of chemical pulp results in an increased density, which implies greater whiteness and smoother surface
- Strength increases with increased amount of chemical pulp

However, it is important to note that these conclusions solely touch virgin fibers and not recycled fibers. In terms of strength, recycled fibers are not stronger than chemical fibers but stronger than mechanical fibers. The greatness in strength of recycled fibers over mechanical fibers is not true in all cases and varies depending on the number of times they have been recycled as well as the pulping method of the virgin fibers (mechanical, chemical, CTMP, etc.). This has to do with the fact that the fibers are shortened each time they are recycled which in turn weakens the fibers. However, recycled fibers do not follow the same trend in density as for virgin fibers. This means that an increase in recycled fibers does indeed increase the strength and density of the paperboard, but does not provide greater whiteness and surface smoothness. [8]

The manufacturing process of paperboard, in which the fiber suspension is deployed onto a moving web and pressed, results in paperboard being anisotropic. This means that paperboard has different mechanical properties in three different directions, as depicted in Figure 4. Starting with the machine direction (MD), which is the direction that the paperboard moves through the machine in the manufacturing process. The cross direction (CD) is the direction that is perpendicular to the MD. And lastly the thickness which is the out-of-plane direction (ZD). The CD and MD are bundled together as the in-plane directions. MD is the direction with the significantly highest stiffness and strength, since MD is the same orientation of the fibers. This is crucial to keep in mind, when planning the conversion and die-cutting of the paperboard or final laminate, since a perforation that tears in the MD direction consequently will have a higher opening force than a perforation that tears in the CD direction. [12-15]

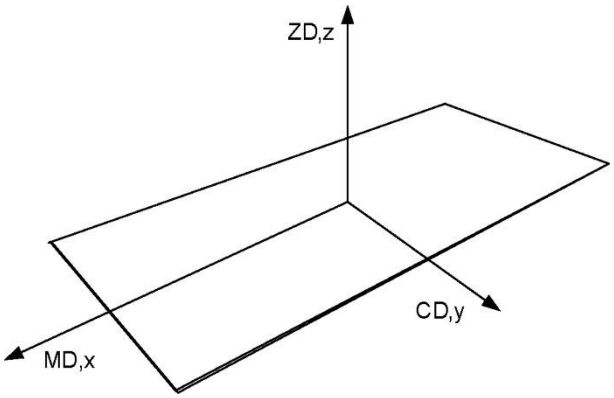

Figure 4. Depicts the material directions of paperboard. In plane directions machine direction (MD), cross direction (CD) and the out-of-plane thickness direction (ZD). [13]

3 Literature Review

As it was mentioned in *Background & Theory*, creasing of body blanks is a vital part of the production process of paperboard packages as without it the folding process would become either impossible or much harder to carry out with satisfying results. However, the knowledge that exists about the creasing process and how it affects the paperboard is understood to some extent as a concept and theory, and often mainly based on empirical studies. Therefore, there is a need for conducting deeper studies in order to obtain knowledge on a deeper level.

Creasing of paperboards depend on the creasing tool parameters in the die-cutting operation and the properties of the paperboard. The paperboard properties include the parameters: material thickness, grammage, and structure. Studies show that thicker materials are able to thin more during creasing, effectively yielding in deeper creases. Furthermore, studies show that even creases with low forming depth reduces the force for folding for all materials. In addition, thinner materials suffers a greater permanent deformation, however folding tests show that creases do not need to be die-cut too fiercely and thus it is possible to achieve desired functionality with less force. [16]

Since the creasing operation and the damage process in material is not understood in great detail, modeling, and simulation by the help of methods such as the finite element method (FEM) are of significant importance.

3.1 Finite Element Analysis of Paper and Paperboard Creasing

Finite element analysis (FEA) is a computer-aided numerical analysis technique involving the finite element method (FEM). Nowadays FEA is a commonly used within a wide variety of engineering design areas, from civil engineering to computational fluid dynamics (CFD), solid mechanics, and automobile engineering among others. Since FEA aids in the prediction, modelling and simulation of how products real-world forces, vibration, stress, and other physical effects, the technique has therefore also been utilized as a tool within the food packaging industry as well. [14]

The purpose of food packaging is to protect the food product from external factors that arise from contaminants, physical damage, and mechanical loadings. Normally, this is tested using a ‘design-prototype-test-redesign’ approach. Although this method of approach is reliable it can also be time-consuming, tedious, and expensive. By utilizing FEA to simulate the structural design of packages, it is possible to develop, troubleshoot, and optimize both current and new designs while at the same time providing savings in both resources and time. By combining FEA with CFD and discrete element method (DEM) it becomes possible to optimize more aspects of the packaging supply chain, such as the performance of packaging in an efficient chilled supply chain and protection of produced goods against damage. [14]

FEA is more specifically used in order to study and understand the material properties of paper and evaluating strength and stiffness properties structural responses [14, 17]. FEA aids in the interpretation of how creasing affects the fiber-structure and the properties of the paperboard in general, in order to better determine the correct die-cutting parameters and also choosing the correct material. Using FEA makes it possible to create stress heat maps that shows which areas and parts of the material that experiences the largest amount of stress. This

further facilitates the designing process of the package and the production process as well [18].

Several authors have conducted an FEA analysis on paperboard creasing and folding [6, 19-22]. Although in almost all these cases the analyzed package design did not include a perforation part close to the creases, a distinctive design for the Boardio® system. In one paper, an FEA was conducted on a packaging material with perforations with the exception of the material being corrugated paperboard and not paperboard, in addition this paper focused on modelling and estimating the compressive strength and not on how the creases affects the material [23].

In a study conducted by Beex and Perlings that focused on paperboard creasing and folding of laminated paperboards it was identified that paperboards with a higher grammage (g/m^2) are harder to convert due to the frequent problem of the top layers breaking. In order to obtain deeper insight and study the paperboard's behavior a mechanical model of FEM is defined that aims to predict the behavior. The developed FE model consists of two models: a continuum model to describe the material and a delamination describing the opening behavior between the different paper plies. All parameters for the models were determined independent experiments of each layer. The developed model revealed that a too shallow crease often resulted in the failure of the top layer. Through the developed model and experimental strain fields it was concluded that apart from the delamination, plastic deformation among the plies in the paperboard must also occur in order for a crease to be considered good as this will prevent the top layer from breaking. [19]

Another approach to study the effect of creasing is to use a laboratory creasing device with equivalent properties of a rotary creasing tool and then to conduct a FEA on the creasing of the paperboard. Once again, the paperboard studied was a multiply paperboard and was modeled as a multilayer structure. In this case the delamination was modeled with a cohesive interface model that connected the paper plies, while the paperboard plies were modeled with an anisotropic elastic-plastic material model. Results conclude that different mechanical properties dominate during the various parts of the creasing operation, however it is mainly shear deformation that causes the delamination during creasing. During the loading part of the creasing operation the shear properties of the paperboard dominates the force-displacement curve. Once loading is complete i.e., displacement is zero and the male die reaches the level of the female die, compression in the thickness direction is important. Another conclusion is that the plies of the paperboard should deform plastically in shear internally. This means that the paperboard is to be constructed so that between the plies there are weak interfaces allowing for easier break of the bonds, but not the fibers. The properties with the biggest influence on the creasing of the paperboard is the out-of-plane shear, out-of-plane compression and the friction between the creasing device and the paperboard. [6]

A general conclusion that can be drawn from the different studies in the area of paperboard creasing analysis using FEM is that the numerical models work provides a good understanding of the behavior of the material during operation and is in some cases also useful for predicting the outcome of the creasing operation [19].

4 Materials & Methods

To assess the material and conversion properties of laminates, proper preparational work needed to be conducted. The preparational work done in this project before examining the material properties were:

- Coordinating raw material supply with the local supply chain department as well as planning trial runs in the tandem extrusion-lamination machine.
- Creating practically applicable technical specifications and laminate recipes for the technical department for trial runs in the tandem extrusion-lamination machine.
- Producing laminate reels according to standard procedure of operations and set technical specifications in the tandem extrusion-lamination machine.
- Sheeting the laminate reels in the correct dimensions in the sheeting machine together with transporting and handling pallets with sheeted laminates according to warehouse standards.
- Coordinating and planning trial runs in the flatbed- and rotary die-cutter together with the local supply chain, engineering, and quality department.
- Coordinating storage of laminate samples, pallets and reels with the local warehouse and logistics department.

4.1 Tensile Strength Measurement

As a general method for evaluating the opening force in the different materials, a Mecmesin MultiTest 2.5-i tensile strength testing machine was utilized. The die-cut body blank was fastened with clamps in the tensile tester, where one of the clamps was in a fixed position and the other clamp is mounted on a force measuring device and able to move with aid from an electric motor, see Figure 5. As the measurement is initiated, the mobile clamp moves in the vertical direction, effectively applying a force to the body blank. The counterforce is perceived by the detector and monitored simultaneously. As the measurement is finished, the mobile clamp returns to its starting position and the test cycle is terminated. To evaluate the corresponding opening force, the maximum applied force, noted in Newton (N), is of interest. To assure statistical significance, ten measurements per position and material was conducted (80 datapoints/material). The force during the test cycle is measured along with the displacement of the upper clamp, creating a force-displacement diagram as can be seen in Figure 6. The figure illustrates a typical cycle curve.

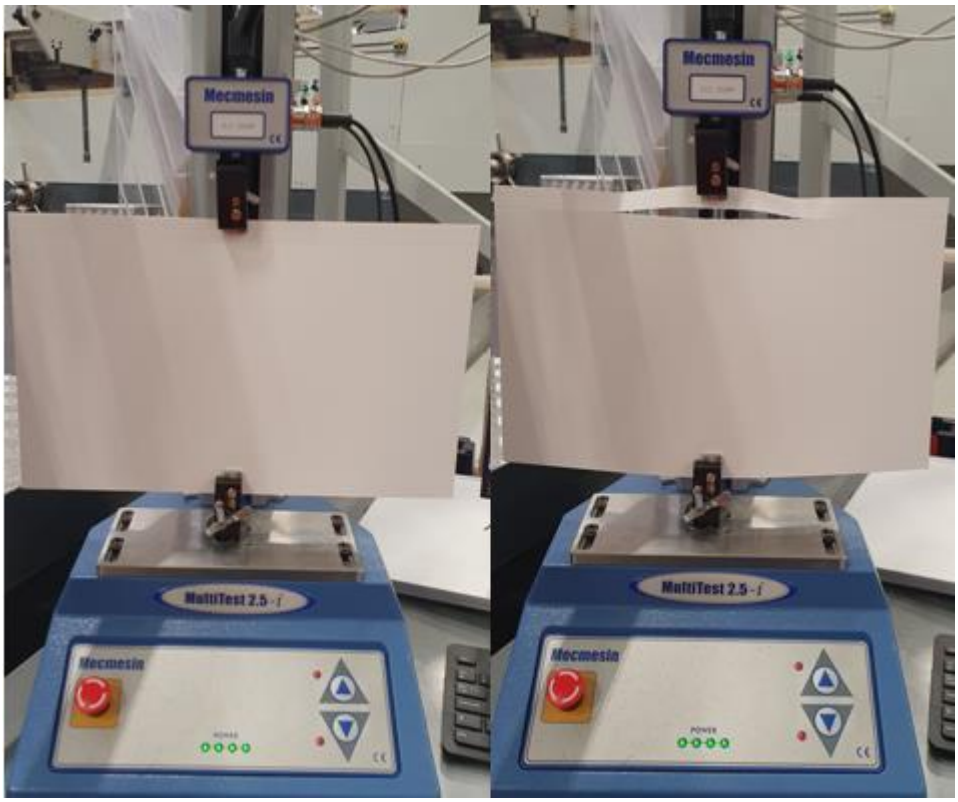

Figure 5. The figure depicts the process of tensile strength measurement of the body perforations.

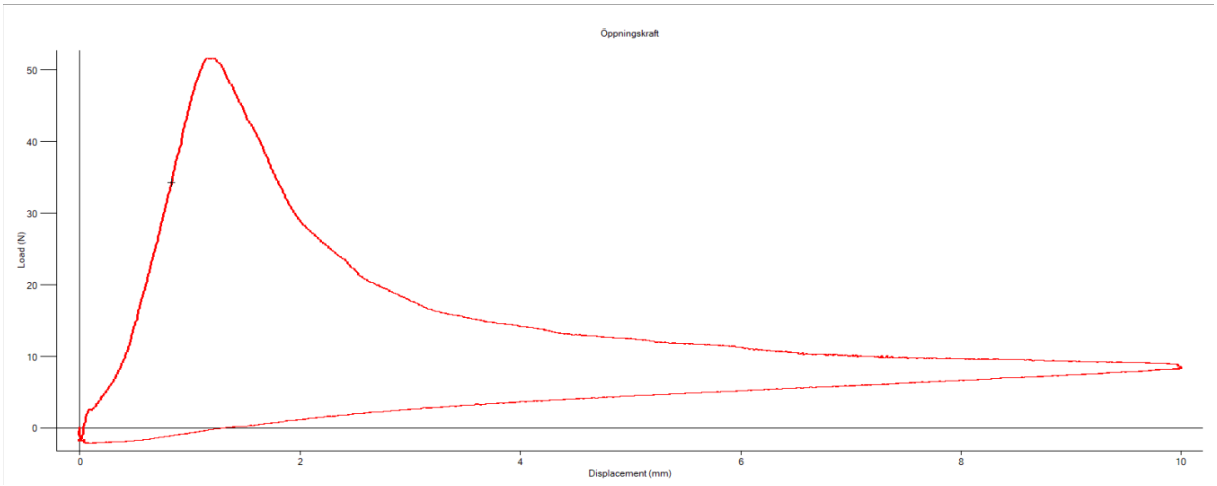

Figure 6. A typical force-displacement diagram acquired in the Mecmesin MultiTest 2.5-i. The exact shape of the curve might change for the different laminates, but the point of interest is still the maximum force noted during one cycle.

4.1.1 Validation

To validate the tensile strength measurements done with material from the flatbed die-cutter, two separate methods of producing perforated laminates was utilized. The first method uses a digital die less cutting and creasing table, commonly referred to as a "plotter," to perforate laminate samples with different perforation sizes, ranging from 0,4 mm to 0,7 mm with 0,1 mm intervals. Samples were prepared of all nine laminates and the opening force was measured for the different laminates. This was done in order to exclude the possibility of fibers in the perforation being damaged or destroyed upon creation of the perforation, which is possible during the die-cutting process due to the immense force applied when the die-cuts the laminates. Further, the isolate effect of the aluminum and PE-film was investigated in this procedure which enables to study how much the separate components contribute to the opening force. The plotter utilizes a sharp cutting tool instead of pressure and a die, and effectively eliminates the possibility of damaging the structural integrity of the components in the laminate.

The second method applied was trial production in a rotary die-cutting machine. The benefits of rotary die-cutting machines are that instead of producing both the creases and the perforation at the same time, the creases are formed first shortly followed by the perforations since the die rotates on the laminate instead of the flatbed action. This can lead to different appearances in both the perforation and the creases when compared to samples from a flatbed die-cutter. For the trial run, only a selection of laminates was produced due to limited equipment access and limitations with regards to the scope of the project. Different configurations were assessed and the opening force for each and every tested laminate and configuration was measured. Further, one sample was also studied in a high-resolution 3D x-ray microscope (see 4.3.2) to compare the effect of the rotary die-cutter with the flatbed die-cutter.

4.2 Crease Thickness Measurement

The die-cut body blank was fed into a thickness measurement device, specifically being a L&W Micrometer (caliper), where nine measurements per body blank was conducted according to Figure 7. The thickness difference between the creased and non-creased part of the body blank was calculated according to:

$$\delta_{pos} = l_{crease} - l_{ref} \quad (1)$$

Pos refers to the position on the body blank being measured, altering from *left*, *middle* and *right* according to Figure 7. How the body blanks are positioned in a laminated sheet is further illustrated by Figure 44 in *Appendix. A – Layout of a Die-cut Sheet.* The measurements are presented in Results and are noted in µm.

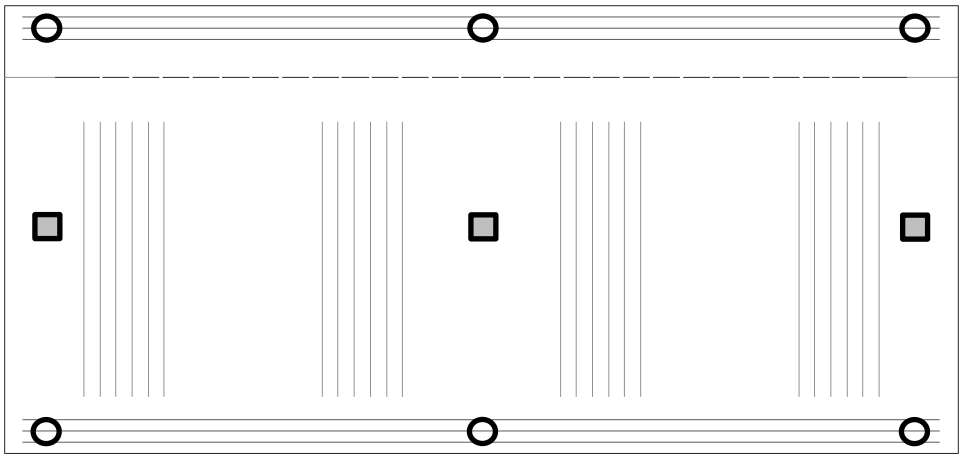

Figure 7. The nine thickness measurement spots are depicted in the figure. The circles are measurements for the creases and the shaded boxes are reference measurements on the non-creased laminate.

In total, three body blanks per position and material was measured (216 measurements/material contributing to a total of 1944 datapoints for all materials).

4.3 Qualitative Analysis

As a complement to the quantitative analysis, the samples were also analyzed with an optic microscope and a high-resolution X-ray microscope.

4.3.1 Optic Microscopy

Both sides of the laminates were examined, being the white clay or bleached paperboard side referred as the outside, and the laminate or polyethylene side, referred to as the inside. Pictures were acquired and can be seen in *Qualitative Results*. The microscope was connected to a camera, acquiring the pictures presented in this report. The magnification was set to 40X.

4.3.2 High-resolution X-ray Microscopy

As a part of the qualitative analysis of the laminates, selected samples were analyzed in a high-resolution X-ray microscope. The machine used was a Zeiss Xradia XRM 520, belonging to the Division of Solid Mechanics at LTH, Lund. The machine works by emitting x-ray beams and measuring the attenuations caused by the substrate, in this case being a paperboard laminate sample. Detectors note the gradual loss of x-ray flux, later enabling computed tomography by combining several images stacked on top of each other to 3D visualize the fibers and layers of the laminates. This serves as a great complement to the optic microscope since the optic microscope essentially only reveals what is observed on the surface of a substrate. Through computed tomography, one can investigate the entire ZD direction of a laminate sample. [24]

The images were acquired with 110kV and 1 micrometer voxel size. In total, 992 images per laminate sample was acquired. Due to the time-consuming sampling and acquirement of images in the Zeiss Xradia XRM 520, only five laminates of most interest were inspected.

4.4 Materials

To evaluate how different laminate structures, behave, three different paperboards together with tree different laminate structures, composing a total of nine laminates, was produced, and assessed. An overview is given in Table 1, and henceforth these denominations will be used.

Table 1. An overview of the different materials produced and assessed.

	Paperboard A	**Paperboard B**	**Paperboard C**
Laminate 1	A1	B1	C1
Laminate 2	A2	B2	C2
Laminate 3	A3	B3	C3

Due to corporate secrecy, the materials will only be described qualitatively, and a fully technical description will not be published. All material specifications and properties were provided in detail by co-supervisor at GPI. The non-disclosure agreement concerns both raw material supplier, raw material and laminate specifications, as well as technical process specifications of the laminate production and conversion. [7]

4.4.1 Laminates

Laminate 1 consists of a paperboard substrate laminated with a polyethylene (PE), together with a thin layer of aluminum foil followed by an extruded PE layer and finished with a thicker layer of PE-film (paperboard/PE/al-foil/PE/PE-film). [7]

Laminate 2 consists of a similar structure as Laminate 1, except that the PE-film is removed (paperboard/PE/al-foil/PE). [7]

In Laminate 3, the al-foil and one PE layer is removed, and the material consist of only PE laminated paperboard (paperboard/PE). [7]

4.4.2 Paperboards

Paperboard A is a complex and multi-layered solid bleached board produced from virgin fibers. It has a high MD bending resistance and a moderate CD bending resistance, a moderate MD and CD bending stiffness, together with a moderate MD and CD tearing resistance. The paperboard is specifically developed to be bent and formed for advanced packaging process applications. [7]

Paperboard B is also a complex and multi-layered board. Two layers consist of unbleached chemical pulp together with a third layer consisting of a bleached chemical pulp. It is solely produced from virgin fibers and has a high MD and CD bending resistance, a high MD and CD bending stiffness, together with a high MD and CD tearing resistance. From the three paperboards investigated, Paperboard B has the highest tearing resistance, bending stiffness and tensile- and burst strength. The paperboard is aimed for high mechanical performance applications where paperboard strength and durability is at outmost importance. [7]

Paperboard C is a more primitive paperboard, produced from virgin fibers. It consists of two layers with sulphate pulp and the third layer being a chemi-thermomechanical pulp (CTMP). It has a low MD and CD bending resistance, low MD and CD tensile strength and a low MD and CD bending stiffness. Unlike paperboards A and B, paperboard C is less mechanically durable and is instead great with regards to foldability and moldability. The paperboard is aimed to fit suitable for packaging process applications where the paperboard is folded. [7]

All paperboards mentioned above, i.e., paperboards A-C are all a part of GPI's commercial product portfolio.

5 Results

5.1 Opening Force Measurements of Flatbed Die-cut Body Blanks

In this section the results from the opening force measurements of all 10 samples conducted on positions 1 to 8 for paperboards A, B & C with all the three different laminates are presented along with summary statistics. The first figure for each laminate showcases how the opening force is spread among the samples and how much it differs from position to position. The second figure for each and every laminate illustrates how the average opening force differs from position to position while at the same time comparing them to the other laminates for each and every paperboard. The testing procedure of opening force was presented in section *Tensile Strength Measurement*. For detailed material composition and configuration (i.e., which paperboard and laminate), see Table 1 in *Materials*.

For all opening force measurements, the data is regarded as randomized. The first data point of position 1 cannot be assumed to originate from the same sheet as the first data point of position 2, and so on. It is also not possible to correlate the order of samples with the order of production in the die-cutter, as the order of measurements in some cases deviate from position to position.

5.1.1 Paperboard A

Figure 8 illustrates spread in opening force within each position as well as the range between lowest and highest measured opening force. It becomes clear that there is not a significant spread present within the all the positions in terms of opening force, except for one measurement in position 8. However, since this data point differs very much from the rest of the group, it could be a possible outlier. The standard deviation and mean opening force for all the measurements is noted in Figure 8. Furthermore, the standard deviation and average opening force for each and every position is summarized in Table 2.

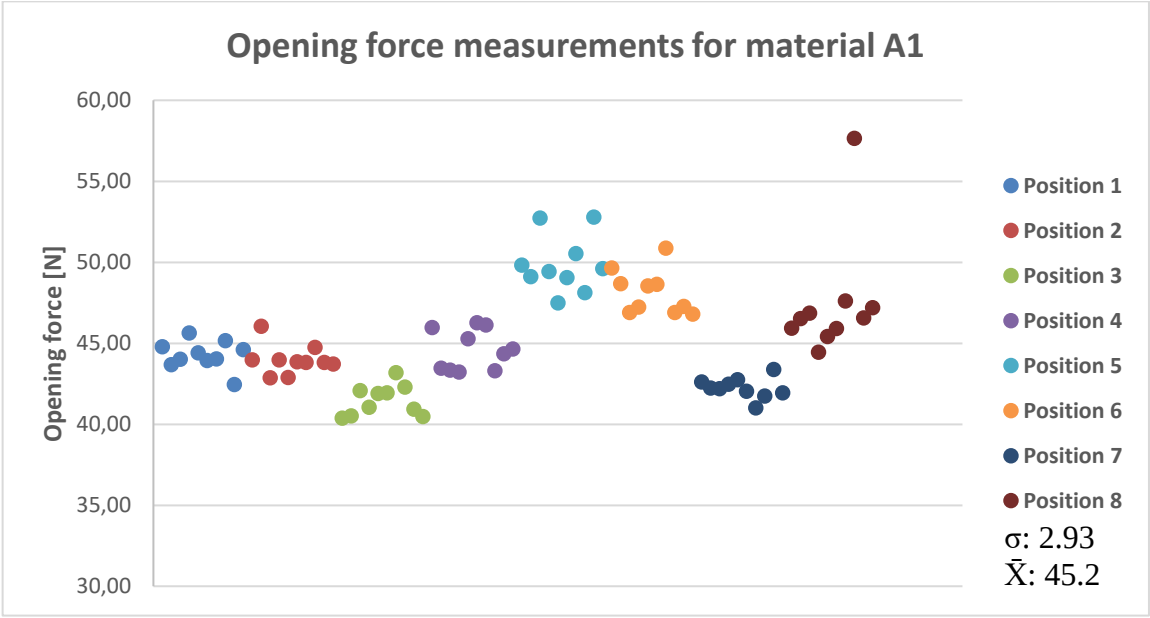

Figure 8. Illustrates the spread in opening force measurements of material A1. The y-axis is the opening force in Newton, required to break the perforations.

Table 2. Summarizes the mean and the standard deviation of the opening force within each and every position for material A1, 1-8, in Newton.

	Position							
	1	**2**	**3**	**4**	**5**	**6**	**7**	**8**
Mean, $\bar{X}$ [N]	44.3	44.0	41.5	44.6	49.9	48.2	42.2	46.7
Std. Dev., σ [N]	0.88	0.91	0.94	1.25	1.74	1.37	0.64	1.49

Figure 9 displays the spread in the opening force measurements of material A2 in and between the various positions. As can be seen in Figure 9, there is a significant spread present in the opening force for material A2. This is true both within each and every position but also between the positions. The lowest measured opening force was 34 N and the highest 53 N. The standard deviation and mean opening force for all the measurements is noted in Figure 9. Furthermore, the standard deviation and average opening force for each and every position is summarized in Table 3.

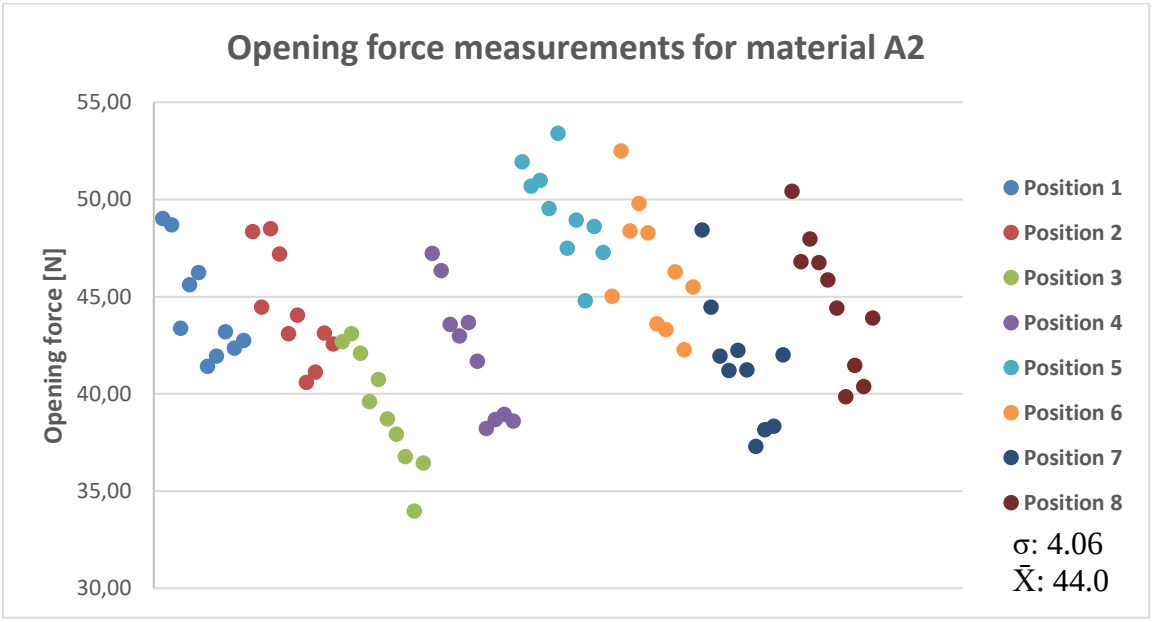

Figure 9. Illustrates the spread in opening force measurements of paperboard A combined with laminate 2. The y-axis is the opening force in Newton, required to break the perforations.

Table 3. Summarizes the mean and the standard deviation of the opening force within each and every position for material A2, 1-8, in Newton.

	Position							
	1	**2**	**3**	**4**	**5**	**6**	**7**	**8**
Mean, $\bar{X}$ [N]	44.5	44.3	39.2	42.0	49.4	46.5	41.5	44.8
Std. Dev., σ [N]	2.77	2.83	3.00	3.31	2.51	3.22	3.28	3.45

The spread in opening force of material A3 looks similair to those of materials A1 and A2 (see Figure 8 and Figure 9) with the only distinction of being intermediately spread out both within and between positions. One clear difference from A1 and A2 is that the opening forces ranged between 59 N at the lowest and 148 N at the highest. The standard deviation and mean opening force for all the measurements is noted in Figure 10. Furthermore, the standard deviation and average opening force for each and every position is summarized in Table 4.

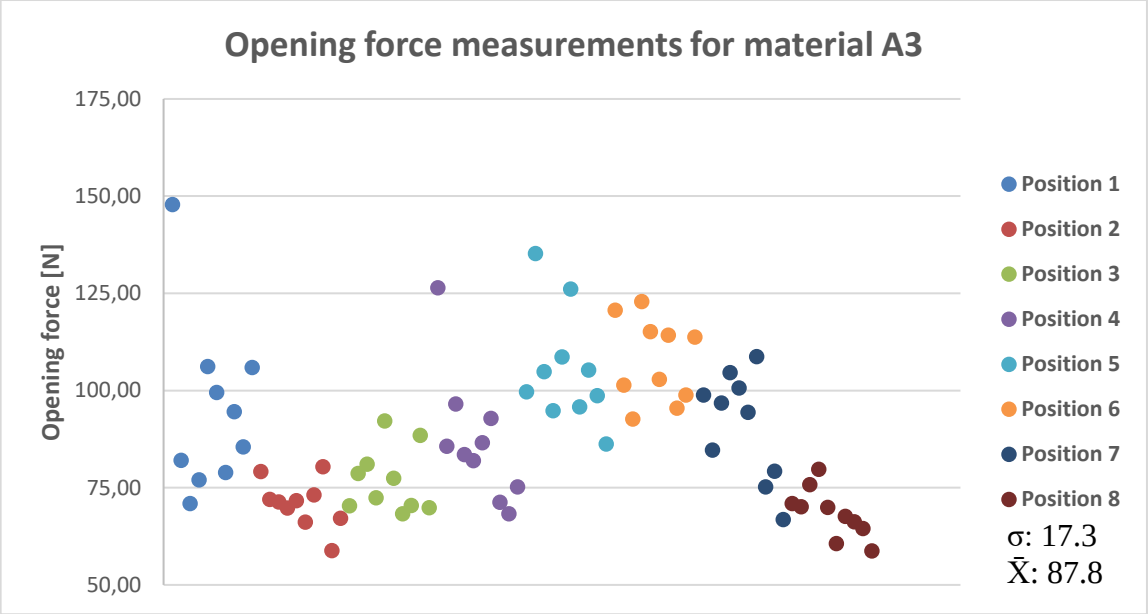

Figure 10. Illustrates the spread in opening force measurements of material A3. The y-axis represents the opening force in Newton, and the x-axis the different positions 1-8.

Table 4. Summarizes the mean and the standard deviation of the opening force within each and every position for material A3, 1-8, in Newton.

	Position							
	1	**2**	**3**	**4**	**5**	**6**	**7**	**8**
Mean, $\bar{X}$ [N]	94.8	70.9	76.9	86.8	105.5	107.8	91.0	68.4
Std. Dev., σ [N]	22.3	6.23	8.27	16.51	14.8	10.8	13.8	6.40

Figure 11 shows the mean opening force for each position in all varied materials and how they are related to each other. All materials, except for A3, have an opening force that is considered to be good enough, however, there also seems to be some kind of pattern present. The mean opening force declines towards the end of the first half of the positions (1-4) in order to then increase, decrease and then once again increase toward the last positions. This pattern was also visible in figures 8-10. The pattern seen here looks identical for materials A1 and A2. Material A3 also follows the same pattern however to a more extreme extent. Another observation that can be made from Figure 11 is that material A3 has an opening force that is notably higher than the averages for materials A1 and A2.

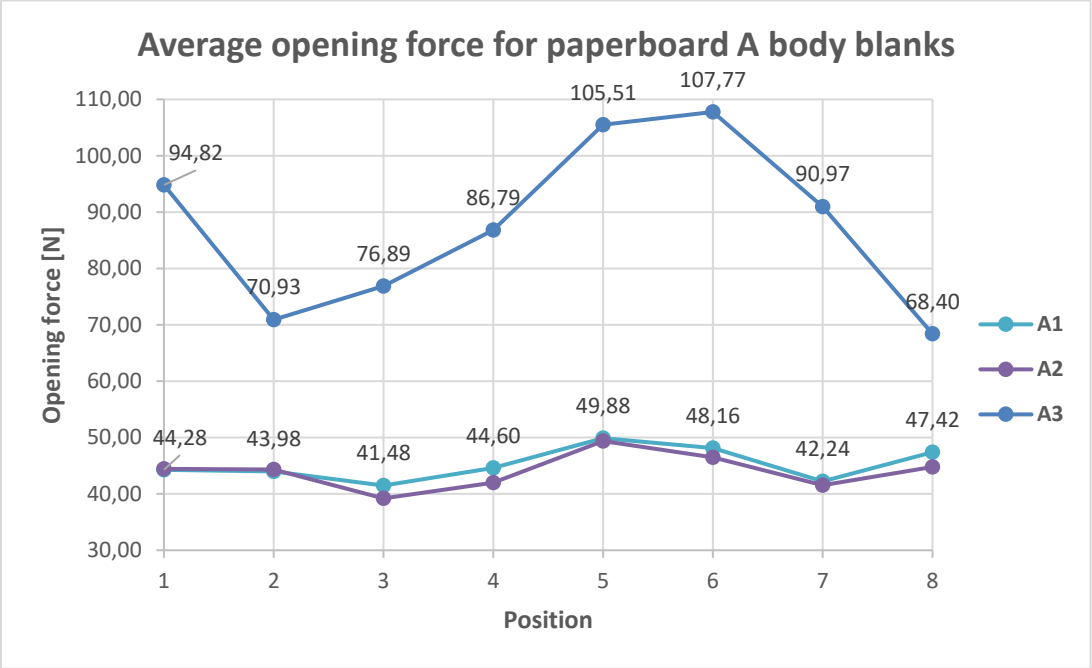

Figure 11. Illustrates how the average opening force measured in Newton differs from position to position for materials A1, A2 & A3. The y-axis represents the opening force in Newton, and the x-axis the different positions 1-8.

5.1.2 Paperboard B

Figure 12 shows an absence in an all too great spread of the opening force for material B1. This is true both within each and every position but also between the positions. The lowest measured opening force was 34 N and the highest 67 N. The standard deviation and mean opening force for all the measurements is noted in Figure 12. Furthermore, the standard deviation and average opening force for each and every position is summarized in Table 5.

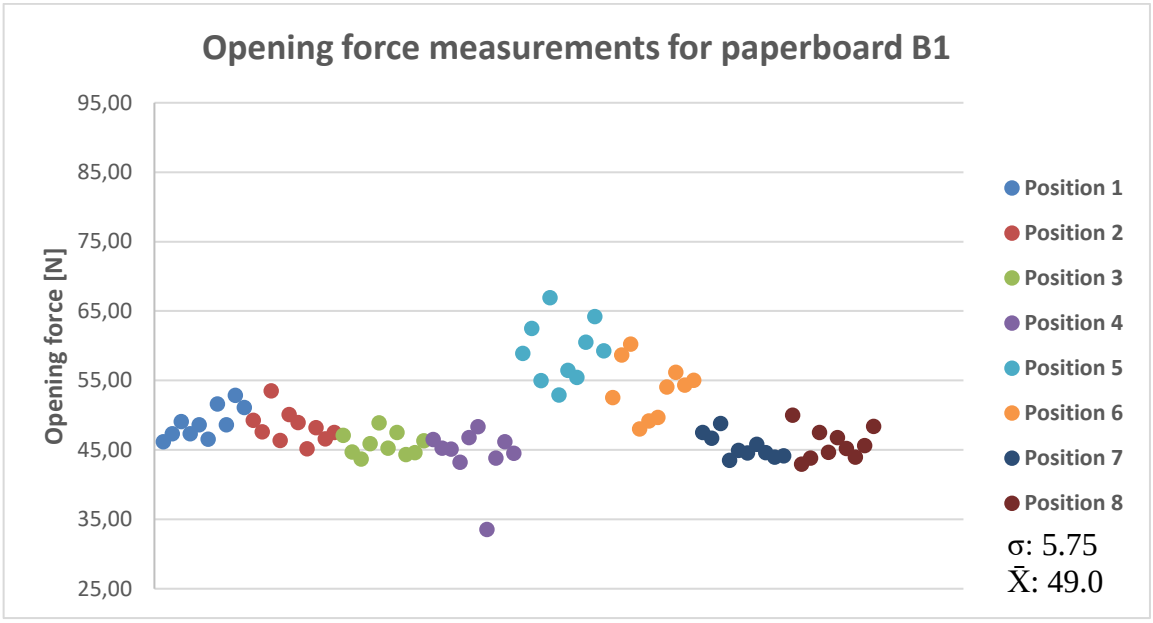

Figure 12. Illustrates the spread in opening force measurements material B1. The y-axis is the opening force in Newton, required to break the perforations.

Table 5. Summarizes the mean and the standard deviation of the opening force within each and every position for material B1, 1-8, in Newton.

	Position							
	1	**2**	**3**	**4**	**5**	**6**	**7**	**8**
Mean, X̄ [N]	48.9	48.3	45.8	44.3	59.2	53.8	45.4	45.9
Std. Dev., σ [N]	2.26	2.34	1.63	4.07	4.43	4.03	1.72	2.25

Figure 13 shows a similar pattern to the one observed for materials A1, A2 and A3, which is the kind of variance of the average opening force between the positions. The largest opening forces was measured at positions 5-6 and the lowest in position 4. Furthermore, all the opening forces measured for material C1 lies withing the acceptable limit.

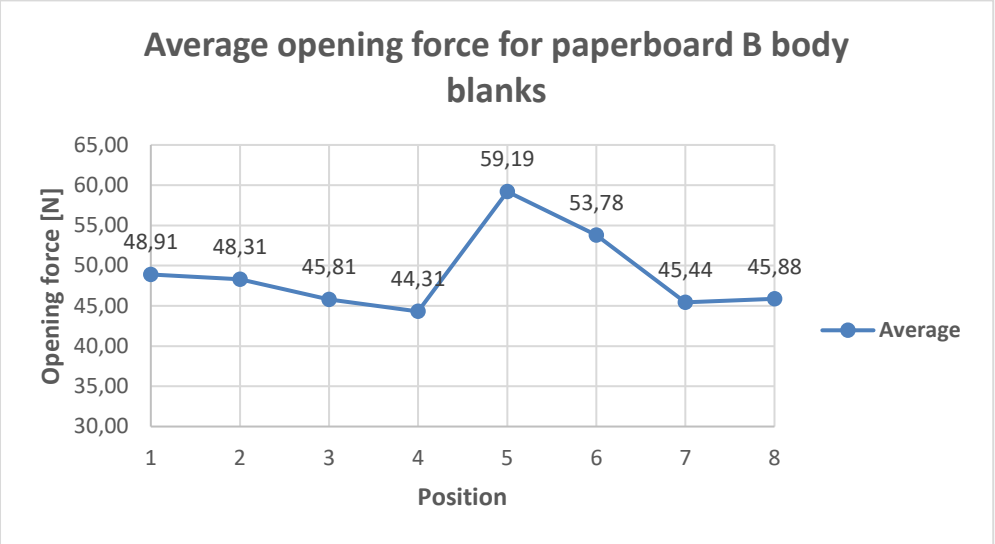

Figure 13. Illustrates how the average opening force measured in Newton differs from position to position for material B1. The y-axis represents the opening force in Newton, and the x-axis the different positions 1-8.

For materials B2 and B3 the same opening force measurements were not possible to conduct. That is because the opening force for these materials were higher than what the testing equipment could handle, which in turn required more powerful equipment. For these materials only two positions were examined (two tests per position) and then it was concluded not to proceed with the rest of the positions, the results from these measurements are summarized in Table 6.

Table 6. Summarizes the mean and standard deviation of the opening force measurements for materials B2 and B3.

		Position	
		1	**8**
Mean opening force [N]	B2	204	133
	B3	165	184

5.1.3 Paperboard C

Figure 14 shows a small spread in the opening force measurement variation within and between positions 1-8 for material C1. The lowest measured opening force was around 31 N while the highest measured opening force was around 41 N. The standard deviation and mean opening force for all the measurements is noted in Figure 14. Furthermore, the standard deviation and average opening force for each and every position is summarized in Table 7.

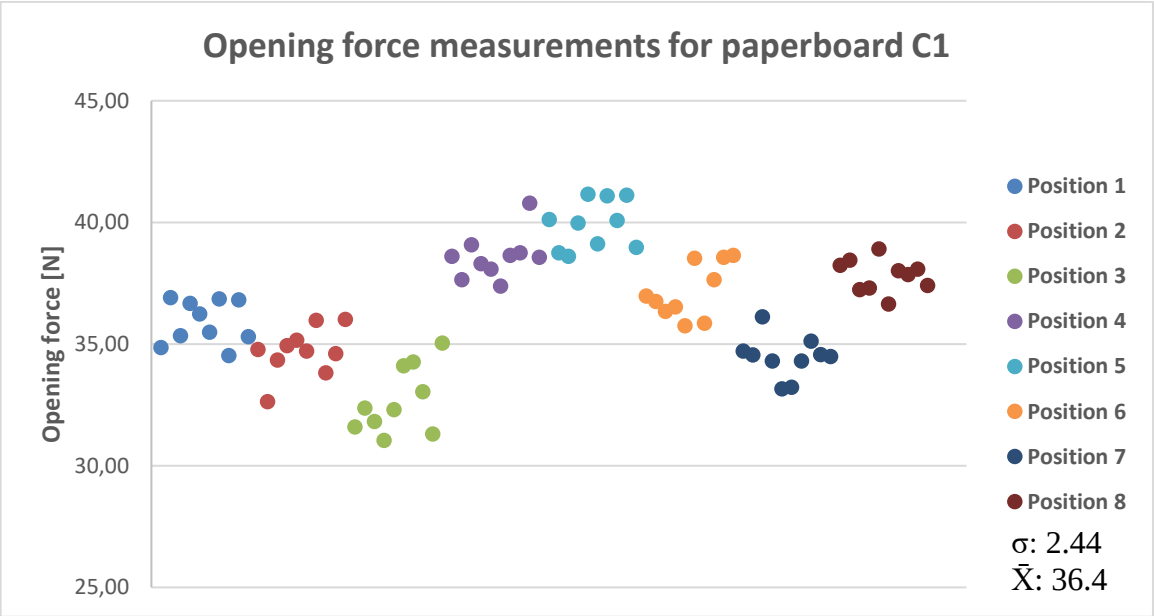

Figure 14. Illustrates the spread in opening force measurements of material C1. The y-axis is the opening force in Newton.

Table 7. Summarizes the mean and the standard deviation of the opening force within each and every position for material C1, 1-8, in Newton.

	Position							
	1	**2**	**3**	**4**	**5**	**6**	**7**	**8**
Mean, X̄ [N]	35.9	34.7	32.7	38.6	39.9	37.2	34.5	37.8
Std. Dev., σ [N]	0.90	0.99	1.37	0.93	1.00	1.12	0.85	0.67

Figure 15 shows the spread in opening force measurements for material C2. In the case of C2, the spread is slightly bigger for some positions when compared to the rest of the positions. There is also a greater range between the lowest and highest measured opening force, with the lowest being 35 N and the highest 70 N. The standard deviation and mean opening force for all the measurements is noted in Figure 15. Furthermore, the standard deviation and average opening force for each and every position is summarized in Table 8.

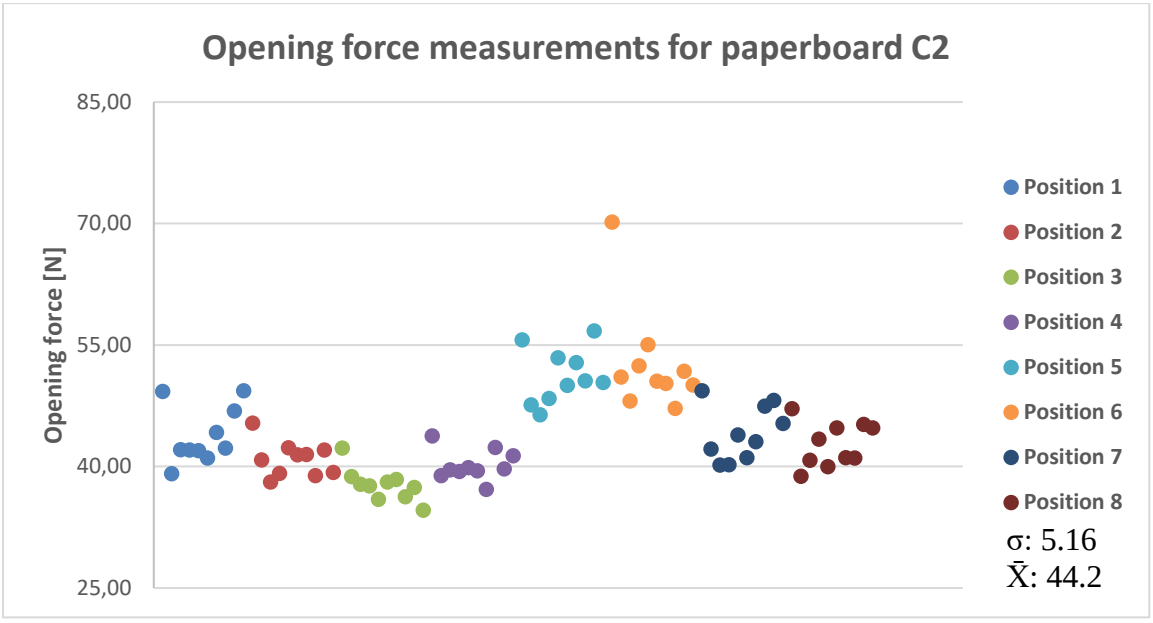

Figure 15. Illustrates the spread in opening force measurements of material C2. The y-axis is the opening force in Newton.

Table 8. Summarizes the mean and the standard deviation of the opening force within each and every position for material C2, 1-8, in Newton.

	Position							
	1	**2**	**3**	**4**	**5**	**6**	**7**	**8**
Mean, $\bar{X}$ [N]	43.8	40.9	37.7	40.1	51.2	52.7	44.1	42.7
Std. Dev., σ [N]	3.52	2.15	2.04	1.87	3.40	6.54	3.36	2.72

In Figure 16 the spread in opening force is illustrated for material C3. In the case of material C3, the spread in opening force differs greatly from position to position. In general, the measurements are not much spread out within the positions, with the exception for positions 5 and 6. In difference from materials C1 and C2, the opening force spread between all positions is also bigger for material C3 with the lowest opening force being 26 N and the highest opening force 94 N. The standard deviation and mean opening force for all the measurements is noted in Figure 16. Furthermore, the standard deviation and average opening force for each and every position is summarized in Table 9.

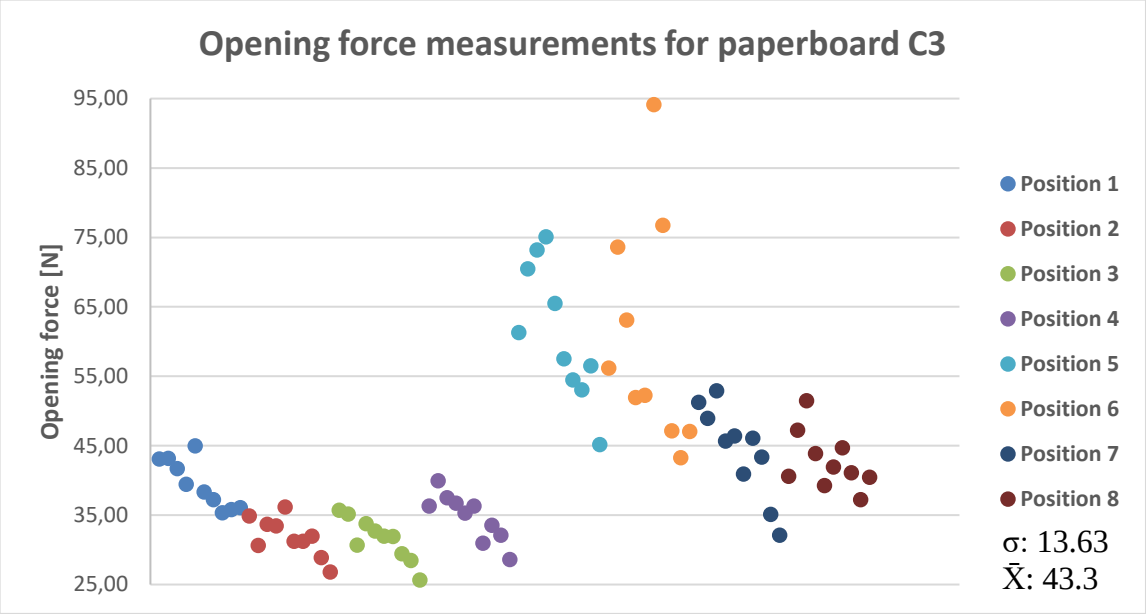

Figure 16. Illustrates the spread in opening force measurements of material C3. The y-axis is the opening force in Newton.

Table 9. Summarizes the mean and the standard deviation of the opening force within each and every position for material C3, 1-8, in Newton.

	Position							
	1	**2**	**3**	**4**	**5**	**6**	**7**	**8**
Mean, X̄ [N]	39.5	31.9	31.5	34.7	61.2	60.5	44.3	42.8
Std. Dev., σ [N]	3.51	2.80	3.09	3.40	9.70	16.30	6.66	4.18

Figure 17 shows the average opening force and how it differs from position to position. In the case of material C1, the average opening force is not considered to be acceptable for positions 2, 3 and 7. However, there is an increase in opening force for positions 4, 5 and 8. When looking at the average opening force for material C2, a familiar pattern reveals itself. That is the pattern of decreased opening force in the first half of the positions (1-4) which turns around and increases towards positions 5 & 6 (51 and 53 N) and ultimately decreases once again to opening forces similar to position 1. In general, all C2 positions have an opening force that is considered to be good enough and acceptable the acceptable range. For the average opening force of material C3 the same pattern is visible as the one seen for materials C1 and C2, however to a greater extent.

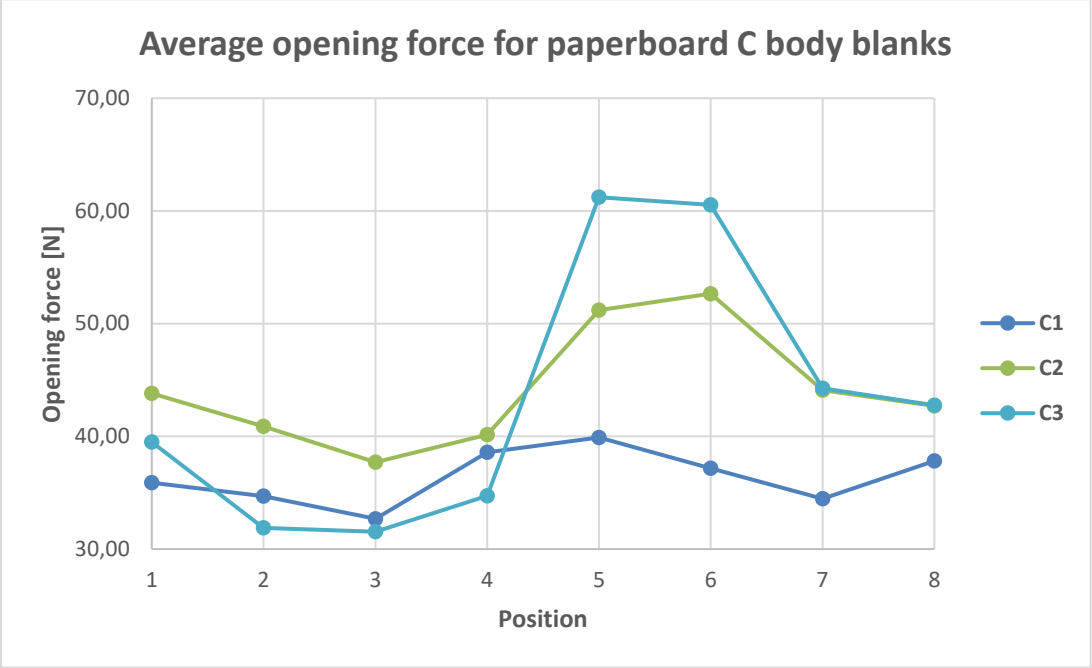

Figure 17. Illustrates how the average opening force measured in Newton differs from position to position for materials C1, C2 & C3. The y-axis represents the opening force in Newton, and the x-axis the different positions 1-8.

5.2 Crease Thickness Measurements of Flatbed Die-cut Body Blanks

Figure 18, Figure 19 and Figure 20 illustrates the average top crease thickness for the different laminates and relates them to the average material thickness. A general trend can be seen that a thinner laminate yields in lower crease height. In general, the crease thickness was noted well below acceptable limits, while the best performing laminate was A1 with respect to crease height. The die-cutter was tuned according to laminate parameters of laminate A1 and kept constant during all trial laminates. The average material thickness and crease height over all positions 1-8 for all paperboards are summarized in Table 10. For the variation in crease height, both top and bottom, over positions 1-8 for all paperboards, see *Appendix. B – Top and Bottom Crease Thickness* Measurements.

Table 10. Summarizes the average thickness along with the average top crease height of all materials, A1-C3, over positions 1-8 in µm.

Average thickness (all positions)

Material	**A1**	**A2**	**A3**	**B1**	**B2**	**B3**	**C1**	**C2**	**C3**
Thickness [µm]	551.7	524.1	504.0	614.2	585.1	566.7	563.1	537.9	511.7
Crease height [µm]	86.39	78.78	52.87	70.44	62.45	46.23	53.60	48.84	30.80

5.2.1 Paperboard A

Figure 18 depicts how the top crease height changes as the material thickness changes. An overall increase in crease height is observed as the material thickness is increased. The biggest increase in crease height is between paperboards A3 and A2 rather than between A2 and A1. However, the increase in material thickness is bigger between paperboards A2 and A1, in difference from the change observed between A2 and A3. The average crease height for paperboard A is showcased in Figure 18.

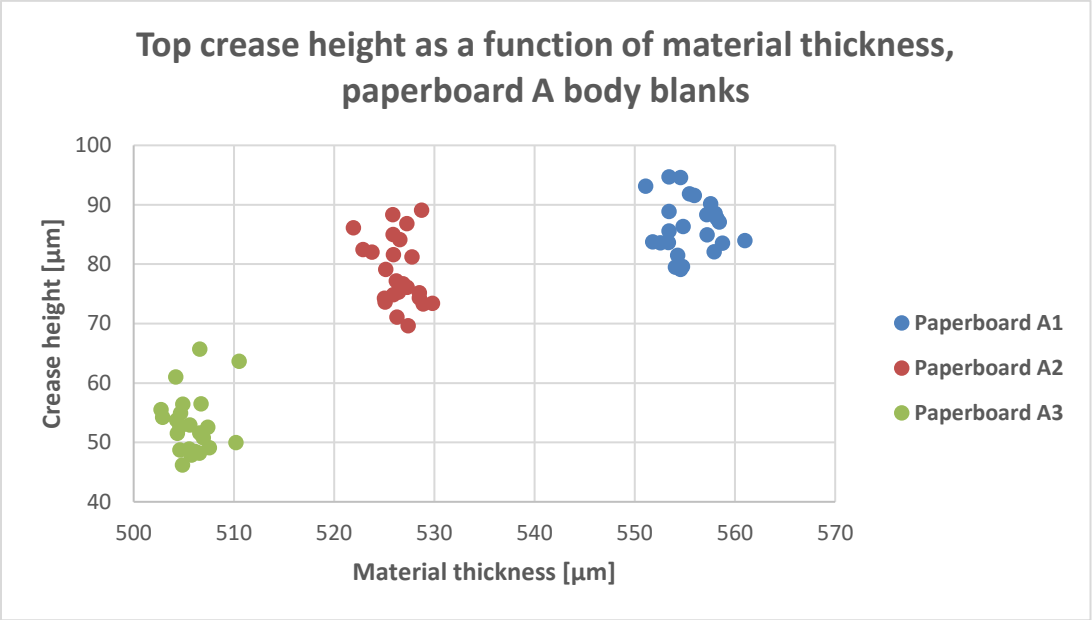

Figure 18. Illustrates the change in crease height as the material thickness increases from paperboard A3 to paperboard A1. The y-axis represents the crease height in µm, and x-axis represents the material thickness in µm.

5.2.2 Paperboard B

Figure 19 depicts how the top crease height changes as a result of change in the material thickness. For paperboard B an overall increase in crease height can be observed as the material thickness increases. The increase in crease height is quite linear between all the different laminates of paperboard B. However, the spread in measurement points is also seen increasing. The average top crease heights for paperboard B is summarized in Figure 19.

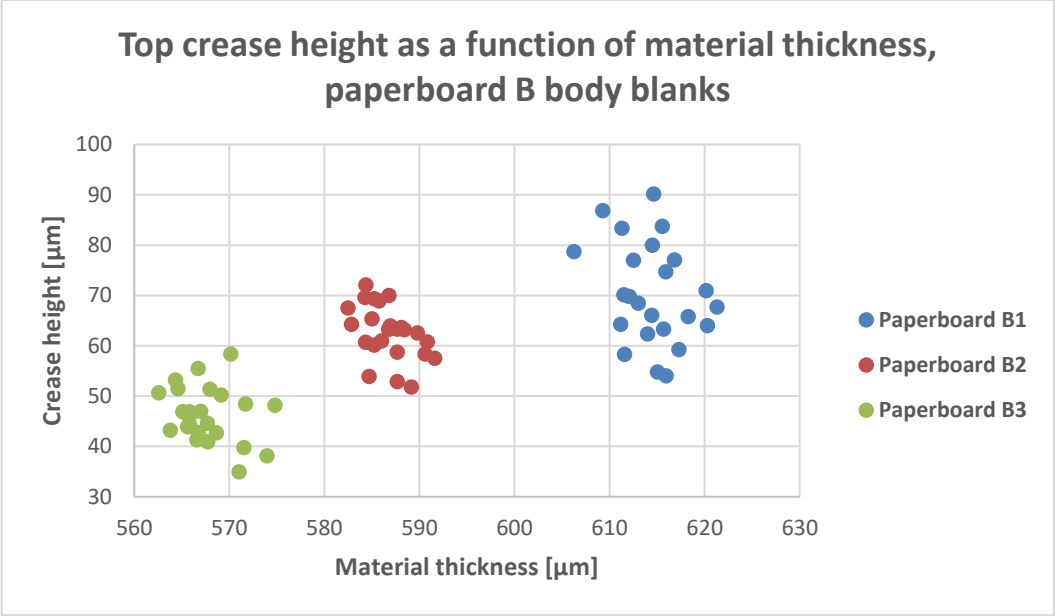

Figure 19. Illustrates the change in crease height as the material thickness increases from paperboard B3 to paperboard B1. The y-axis represents the crease height in µm, and x-axis represents the material thickness in µm.

5.2.3 Paperboard C

Figure 20 depicts how the top crease height changes as a result of change in the material thickness. For paperboard C an overall increase in crease height can be observed as the material thickness increases, the increase in material thickness seems to be quite the same between all laminates. Changes in crease height are more significant between paperboards C3 and C2 than between C2 and C1. The average top crease height for paperboard C is summarized in Figure 20.

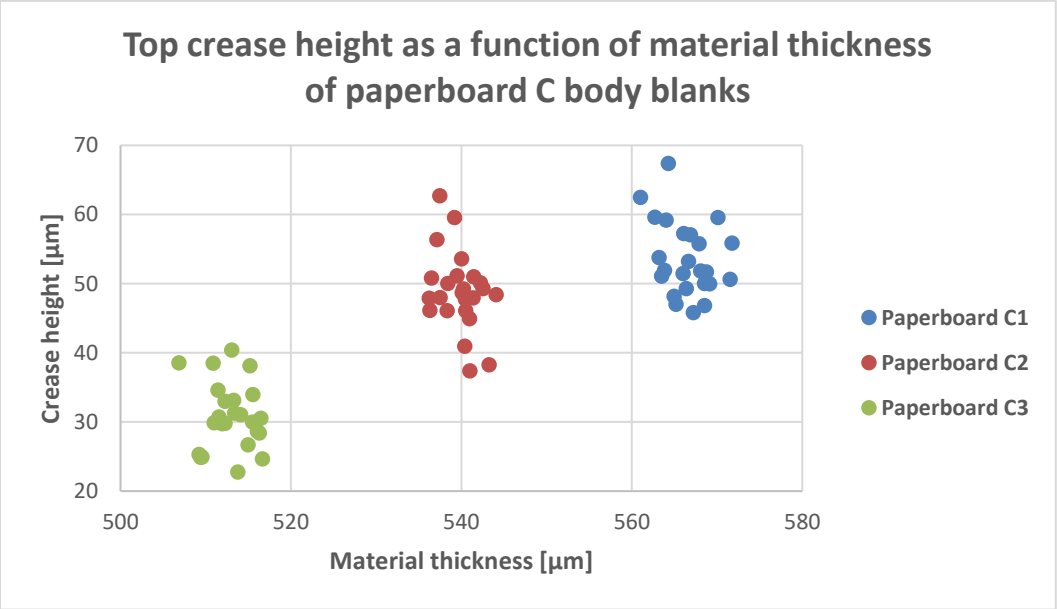

Figure 20. Illustrates the change in crease height as the material thickness increases from paperboard C3 to paperboard C1. The y-axis represents the crease height in µm, and x-axis represents the material thickness in µm.

5.3 Possible Correlation Between Crease Thickness and Opening Force

The results from the first crease thickness and opening force measurements (see sections 5.1 and 5.2) indicated the presence of a possible correlation between crease thickness and opening force. Therefore, opening force and crease thickness measurements were conducted once again. Though this time the two tests were done on the same sample and only for paperboard A, since the die-cutter along with its parameters were initially tuned after paperboard A.

The results from the paired sample measurements of opening force and crease height are in short summarized in Table 11, which shows an increase in the mean opening force as the amount of laminate component decreases while at the same time the mean crease height decreases as the amount of laminate component decreases. At a first glance, this suggests that there could be a correlation between opening force and crease height.

Table 11. Showcases how the mean and standard deviation of the opening force and crease height differs between the different laminates of paperboard A.

	A1	**A2**	**A3**
Mean of opening force [N]	44.4	52.8	75.4
Standard deviation of opening force [N]	3.06	4.18	17
Mean of crease height [µm]	85.3	80.5	53.1
Standard deviation of crease height [µm]	6.21	6.73	6.48

Figure 21 showcases a scatterplot of the opening force on the x-axis against crease height on the y-axis and it appears that there may be a negative relationship between the crease height and the opening force. This means that obtained data from the paired tests initially indicate that the thicker the laminate is, the easier the final packaging will be to open.

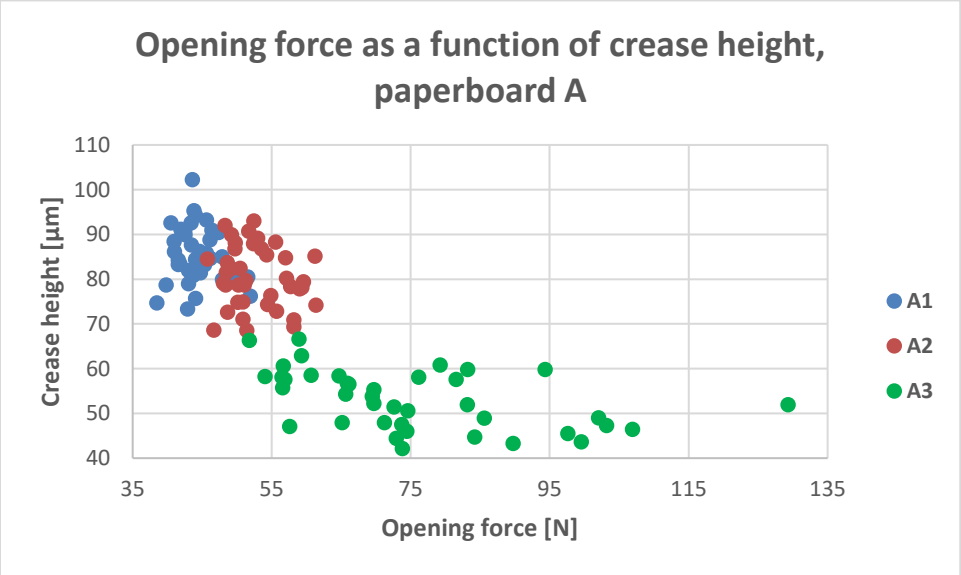

Figure 21. Illustrates a scatterplot of the opening force and the crease height and indicates the presence of a possible relationship between the two variables for the different laminates. The y-axis represents the crease height in µm and the x-axis the opening force in Newton.

Figures 22-24 illustrates individual scatter plots for laminates A1, A2, and A3. Furthermore, it is observable, when studying the laminates individually, that the presence of a pattern between opening force and crease height is not as certain as it is illustrated by Figure 21.

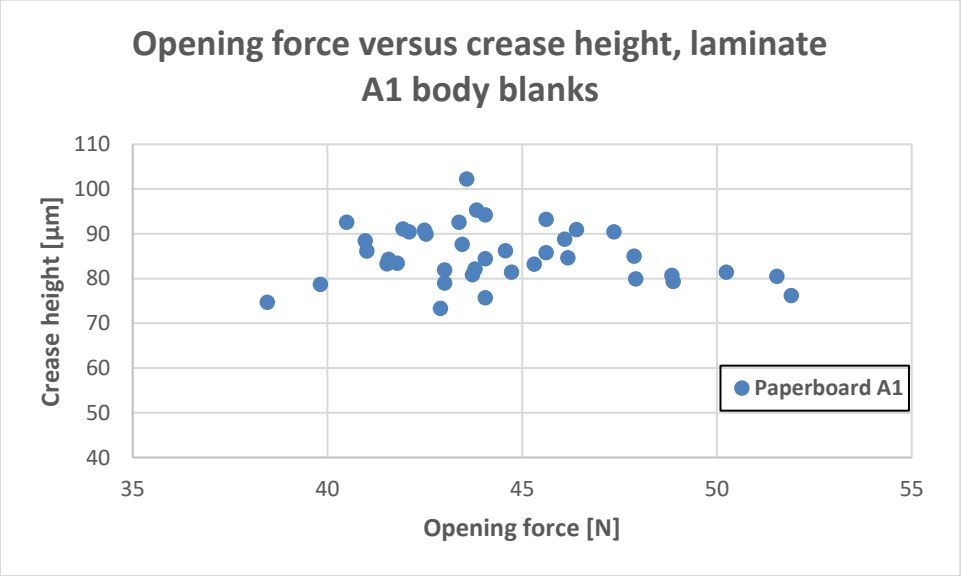

Figure 22. Illustrates a scatterplot of the opening force versus the crease height for laminate A1 body blanks. The y-axis represents the crease height in µm and the x-axis the opening force in Newton.

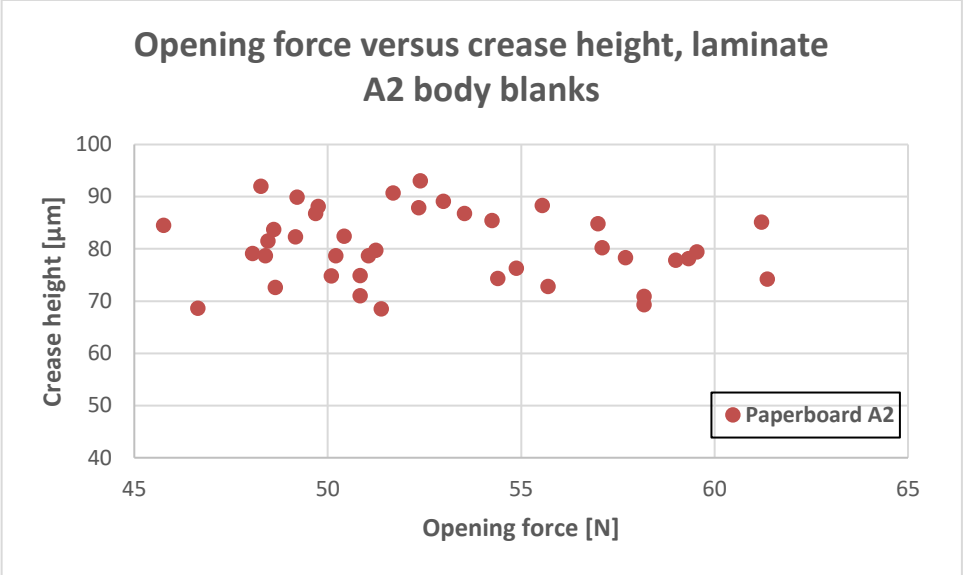

Figure 23. Illustrates a scatterplot of the opening force versus the crease height for laminate A2 body blanks. The y-axis represents the crease height in µm and the x-axis the opening force in Newton.

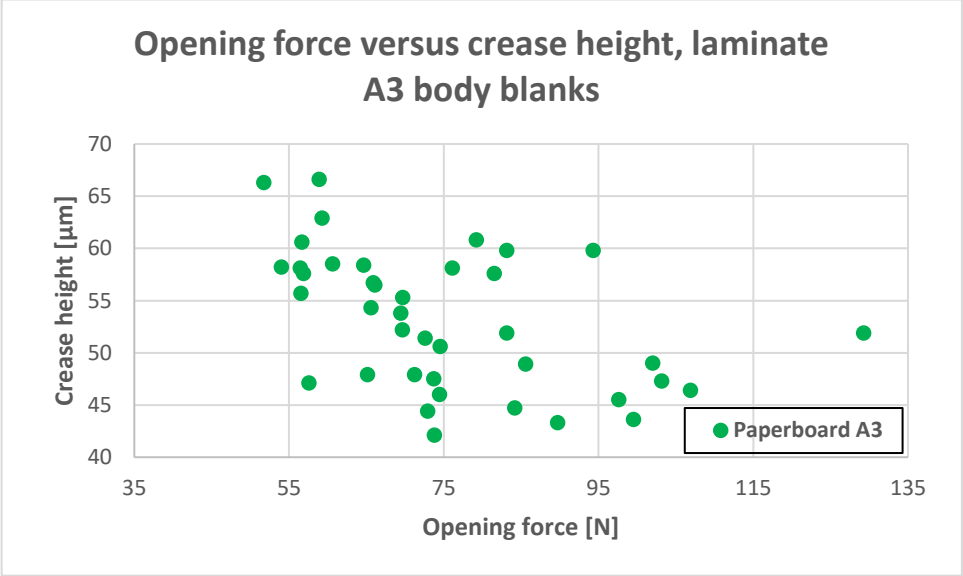

Figure 24. Illustrates a scatterplot of the opening force versus the crease height for laminate A3 body blanks. The y-axis represents the crease height in µm and the x-axis the opening force in Newton.

5.4 Plotter Results

As mentioned in section 4.1.1, the tensile strength measurements were conducted once again to better understand how the flatbed die-cutter affects the laminates. In addition, it was desired to identify how much each addition of a new component, i.e., the al-foil, PE, and PE-film, in every laminate contributed to the opening force of the laminates. Lastly, the purpose of the extended tensile strength measurements allowed for looking into and comparing alternative perforation sizes and configurations as well.

5.4.1 Tensile Strength Measurements on Plotted Samples

In the plotter tests, all paperboards and laminates were tested with different perforation sizes ranging from 0.4 to 0.7 mm with a 0.1 mm interval. The perforation configuration looked like the perforations are depicted in Figure 3, while the test samples did not include any creasing lines and were smaller in size than that of Figure 3. The results of paperboard A from the plotter tests are depicted in Figure 25, in which a general increase in opening force is visible as the perforation size increases. This is true for all laminates of paperboard A. However, for some reason, 0.5 mm sized perforations seem to yield in a higher opening force than 0.6 mm sized perforations, this is especially true for paperboards A1 and A2. In the case of paperboard A1, the 0.5 mm sized perforation is the strongest perforation. In general, it can be concluded from Figure 25 that the average opening force increases with increased number of components in the laminate along with the perforation sizes.

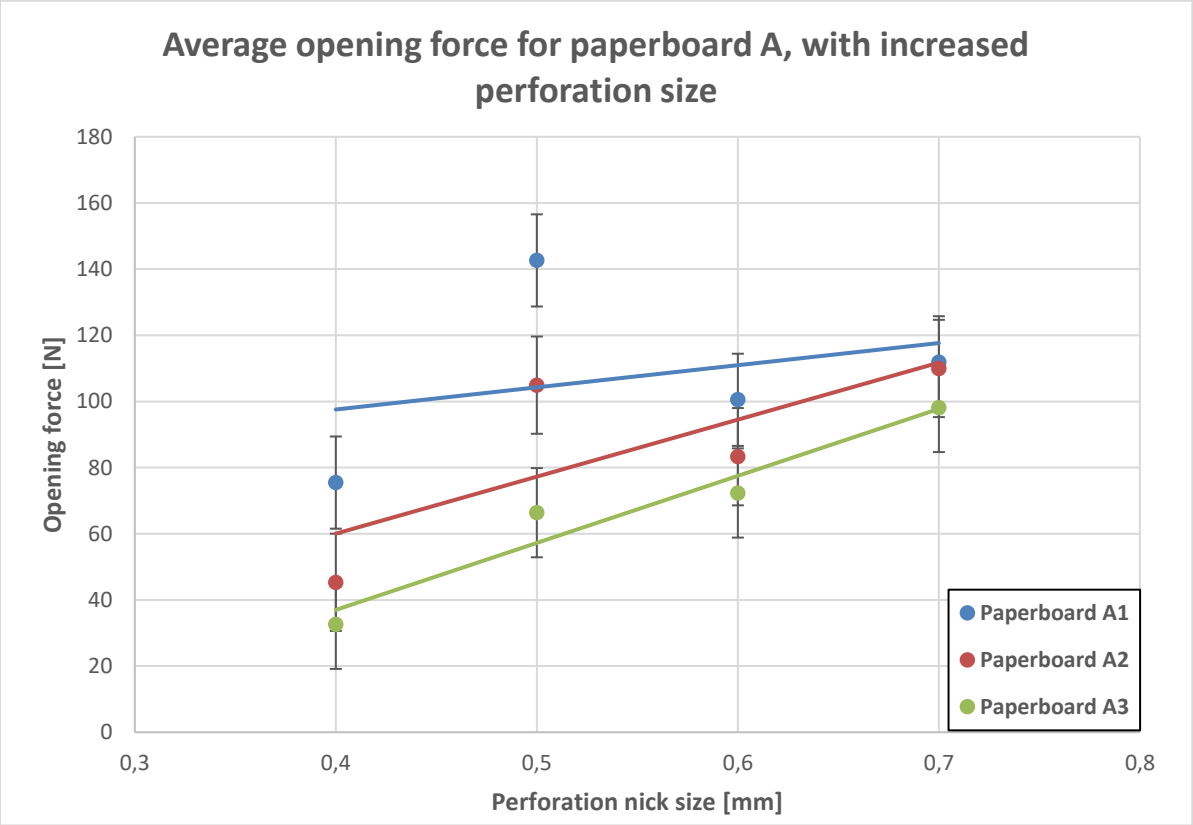

Figure 25. Illustrates how the average opening force increases with increased perforation size and how the average opening force differs for the different laminates of paperboard A. The y-axis represents the opening force in N and the x-axis represents perforation size in mm.

Figure 26 showcases the change in opening force because of increased perforation size, while at the same time comparing the different laminates of paperboard B with one another. The opening force increases because of the increased perforation size. Once again, there is a significant increase between the 0.5 mm and 0.4 mm sized perforations so that the 0.5 mm sized perforation has a higher opening force even than the 0.6 mm sized perforation. Although Figure 26 shows quite similar opening force for the paperboards B2 and B3, there is a bigger difference between them and paperboard B1.

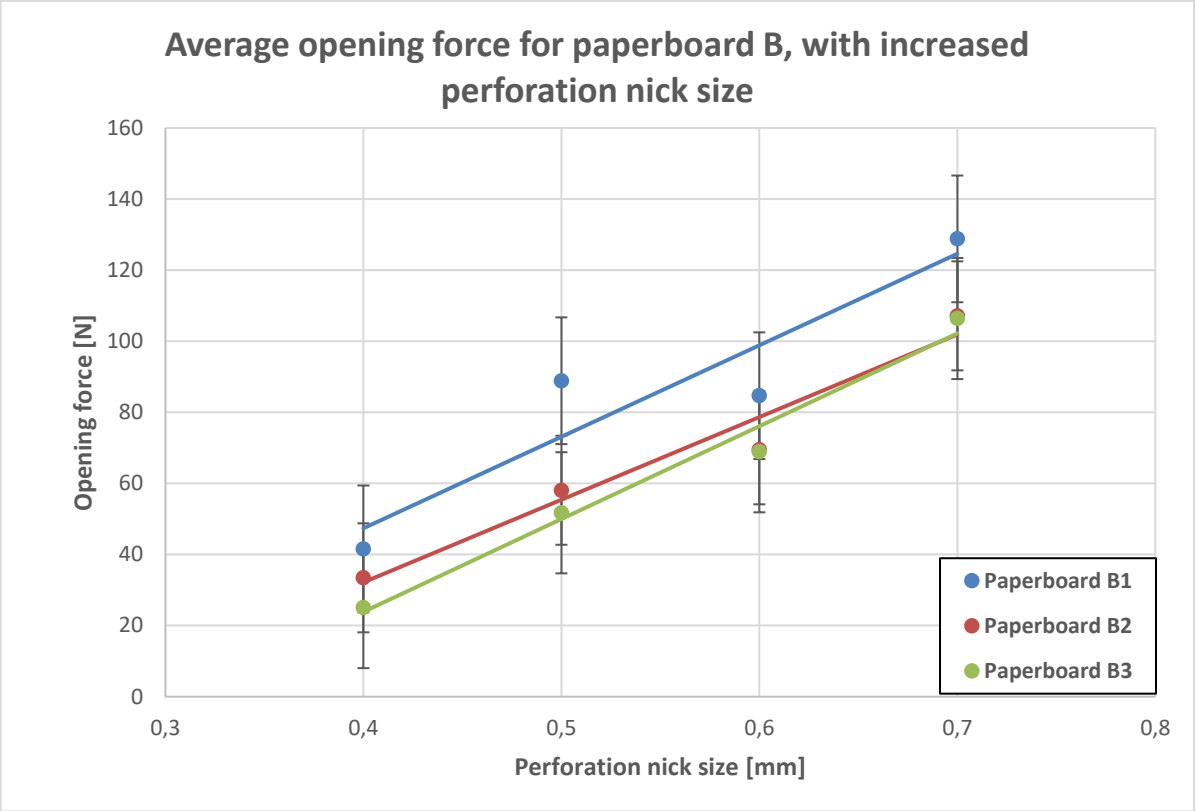

Figure 26. Illustrates how the average opening force increases with increased perforation size and how the average opening force differs for the different laminates of paperboard B. The y-axis represents the opening force in N and the x-axis represents perforation nick size in mm.

Figure 27 showcases the difference in opening force for paperboard C as the perforation sizes and the number of components in the laminate increases. An increase in perforation size results in an increased opening force even for the case of paperboard C. Furthermore, the more components the laminate consists of, the higher the opening force gets, this is especially true for paperboards C2 and C3. Paperboard C1 shows a great increase in opening force when the perforation size is increased from 0.4 to 0.5 mm.

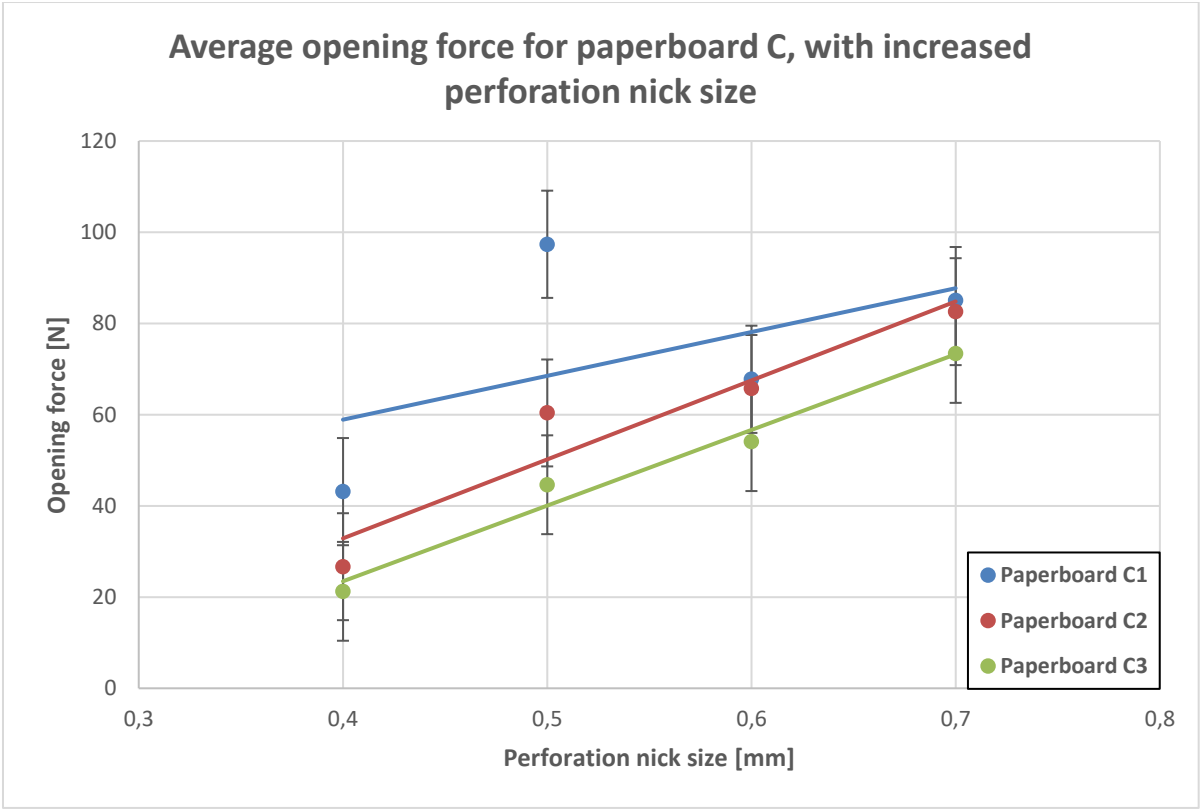

Figure 27. Illustrates how the average opening force increases with increased perforation size and how the average opening force differs for the different laminates of paperboard C. The y-axis represents the opening force in Newton and the x-axis represents perforation nick size in mm.

Figure 28 provides an overview and facilitates the understanding of how much the average opening force is affected by the addition of al-foil, PE, and PE-film. The biggest contributions are done to paperboard A, while the smallest for paperboard B.

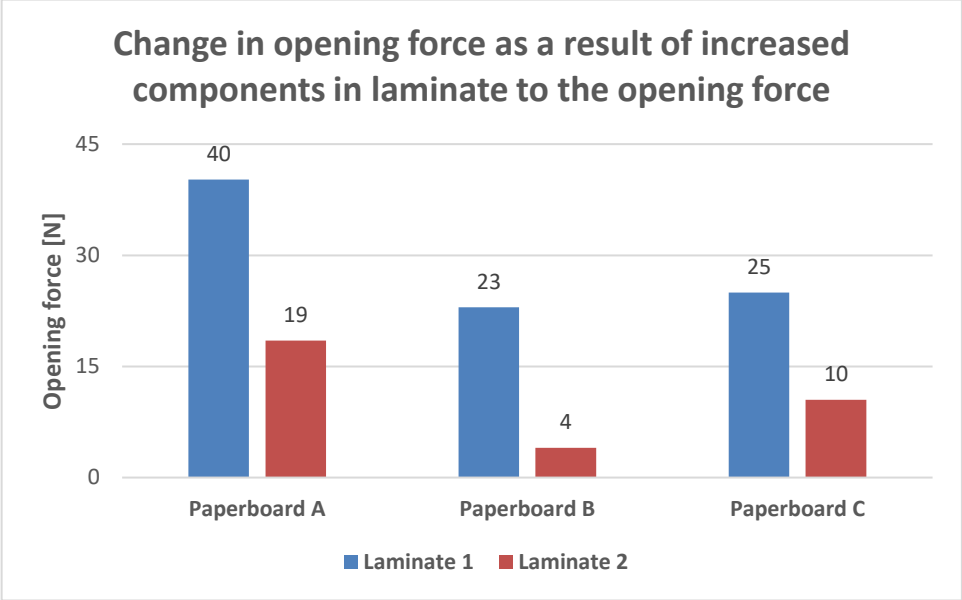

Figure 28. Illustrates how the average opening force increases with the subsequent addition of al-foil, PE, and PE-film for all paperboards and how the average opening force differs for the different laminates of paperboard C. The y-axis represents the change in opening force in Newton and the x-axis represents the different paperboards.

On average, the addition of al-foil and PE to the laminate results in an 11 N increase of the opening force, while the addition of al-foil, PE and PE-film results in an increase of 29 N. Thus, it can be concluded that the PE-film contributes with 18 N to the opening force in the ideal case, i.e., when the body blanks are not creased and only perforated.

In addition, the perforation of the plotted samples were made up of 8 nicks and Table 12 illustrates the perforation strength in N/mm nick for all laminates.

Table 12. Summarizes the perforation strength in Newtons/mm for all laminates and perforation configurations of the plotter.

		Perforation strength [N/mm]			
		Nick size [mm]			
		0,4	***0,5***	***0,6***	***0,7***
Laminate	A1	23,6	35,7	20,9	20,0
	A2	10,2	26,2	17,4	19,6
	A3	10,2	16,6	15,1	17,5
	B1	13,0	22,2	17,6	23,0
	B2	10,4	14,5	14,5	19,1
	B3	7,8	12,9	14,4	19,0
	C1	13,5	24,3	14,1	15,2
	C2	8,3	15,1	13,7	14,7
	C3	6,6	11,2	11,3	13,1

5.5 Rotary Die-Cutter Results

Since the parameters of the flatbed die-cutter were tuned according to laminate A1, only laminates of paperboard A were investigated in the rotary die-cutter. In addition, the rotary die-cutter allowed testing other perforation sizes as well and ultimately led to the production of body blanks of paperboard A with perforations sizes ranging from 0.6 to 0.9 mm. Figure 29 depicts the change in opening force of rotary die-cut of paperboard A body blanks. The figure shows similar opening forces for paperboards A1 and A2 with a clear pattern, which is the increase in opening force because of increased perforation size. The increase in opening force due to bigger perforations is true for all laminates of paperboard A. One behavior that also is common for all laminates is the fact that 0.7 mm sized perforations yield in higher opening force than both 0.6- and 0.8-mm sized perforations.

Furthermore, it is also interesting to study the scatterplots of the opening forces of rotary die-cut paperboard A laminates. These are showcased by Figure 30, Figure 31 and Figure 32. In general, it can be concluded that no laminate of paperboard A performs better than the other in terms of the spread in data points. Nick sizes are comparable to the sizes of commercial production.

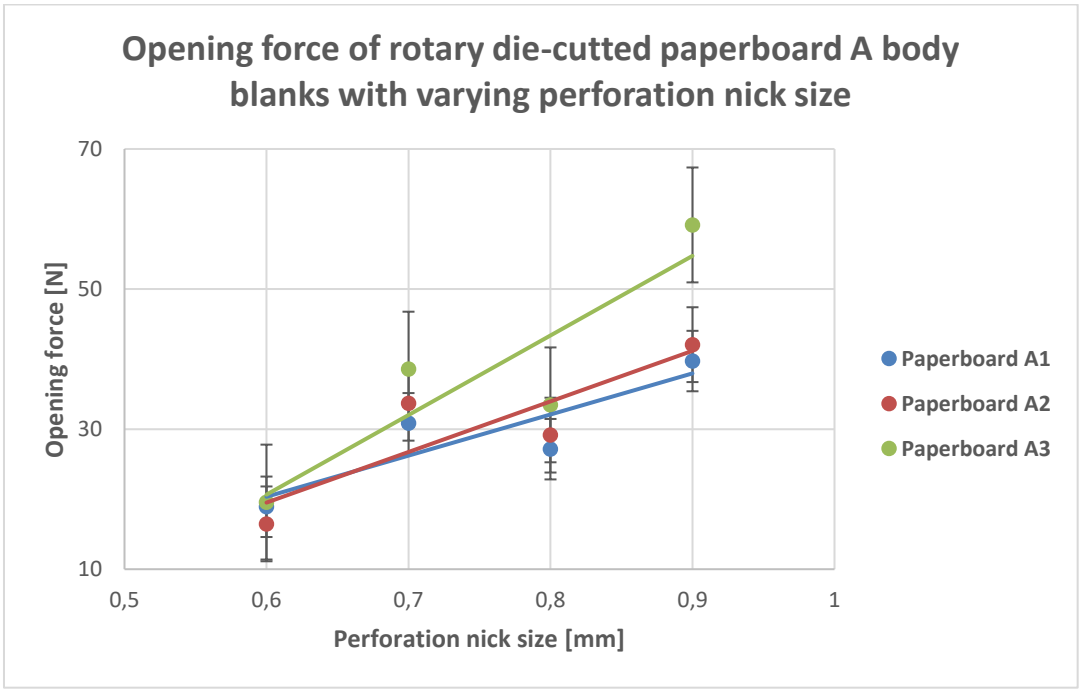

Figure 29. Illustrates the average opening force of rotary die-cut body blanks of paperboard A along with the change in perforation nick size. The y-axis represents the opening force in Newton, and the x-axis the perforation size in mm.

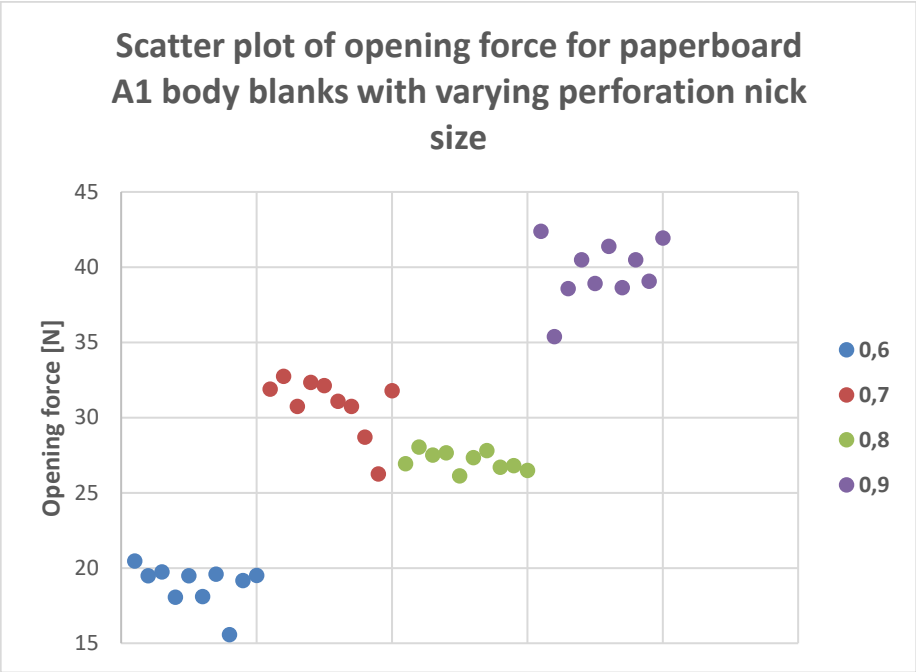

Figure 30. Illustrates the spread in the opening force of paperboard A1 rotary die-cut body blanks. The y-axis represents the opening force in Newtons and the different perforation nick sizes are color coded.

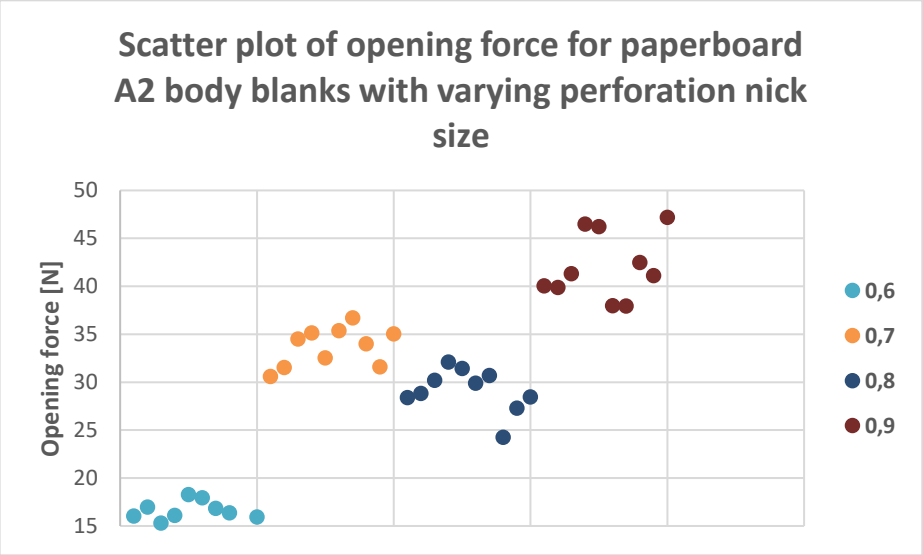

Figure 31. Illustrates the spread in the opening force of paperboard A2 rotary die-cut body blanks. The y-axis represents the opening force in Newtons and the different perforation nick sizes are color coded.

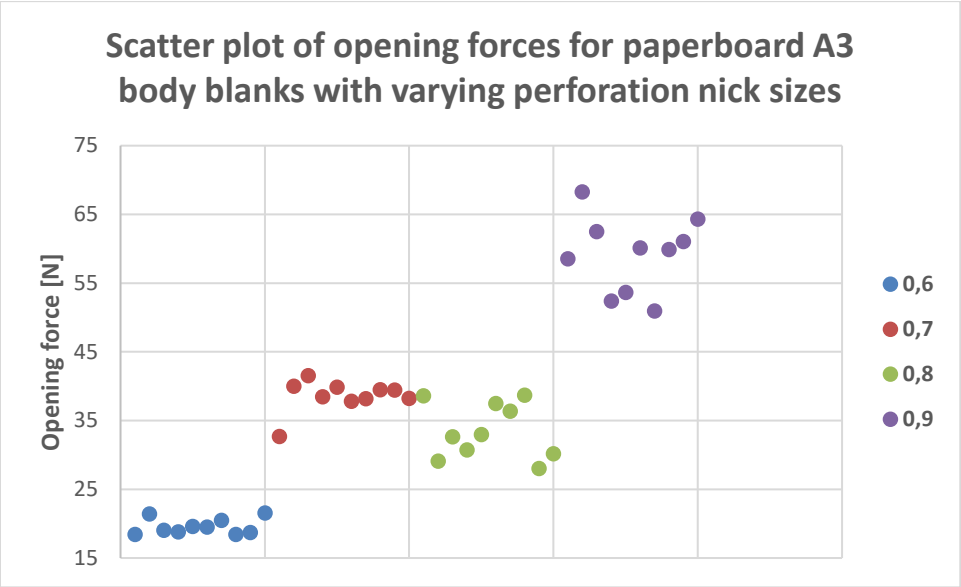

Figure 32. Illustrates the spread in the opening force of paperboard A3 rotary die-cut body blanks. The y-axis represents the opening force in Newtons and the different perforation nick sizes are color coded.

5.6 Qualitative Results

5.6.1 Optical Microscope

The acquired images of the different laminates are presented below in the order of paperboard A, outside (Figure 33), paperboard A, inside (Figure 34), paperboard B, outside (Figure 35), paperboard B, inside (Figure 36), paperboard C, outside (Figure 37), and paperboard C, inside (Figure 38). All images were acquired with magnification 40X. The perforation examined was chosen to the most middle one on a die-cut body blank and was consistent over all samples. A backlight was applied, which can be seen as a white light in the cut between the perforations. The backlight acts as an aid to showcase how well cut the laminate is and to highlight if the perforation is of sufficient thickness, since it otherwise would be partially translucent.

A general tendency was observed, being that a thicker laminate with more components yielded a greater degree of destruction in the fibers of the outermost layers in the paperboard. It is crucial to emphasize that only qualitative results with regards to the observable outermost layers of the paperboard can be noted, since optical microscopy is a topographic method and does not study the integrity of the material such as a tomographic method would do. Further, a general tendency with regards to the laminate side was also observed, being that a thicker laminate with more components yielded a greater destruction in the aluminum foil. In laminates A2, B2 and C2, the aluminum foil can be seen only partially torn apart. In laminates A1, B1 and C2 however, the aluminum layer is entirely torn apart.

Figure 33 and Figure 34 shows the perforation of paperboard A, being the paperboard with intermediate to high durability and strength compared to the other paperboards in this study. As noted, before, the rupture in the outermost layer of the paperboard and the aluminum layer is worst in A1, followed by A2 still being thoroughly torn apart, and A3 only having a partial rupture.

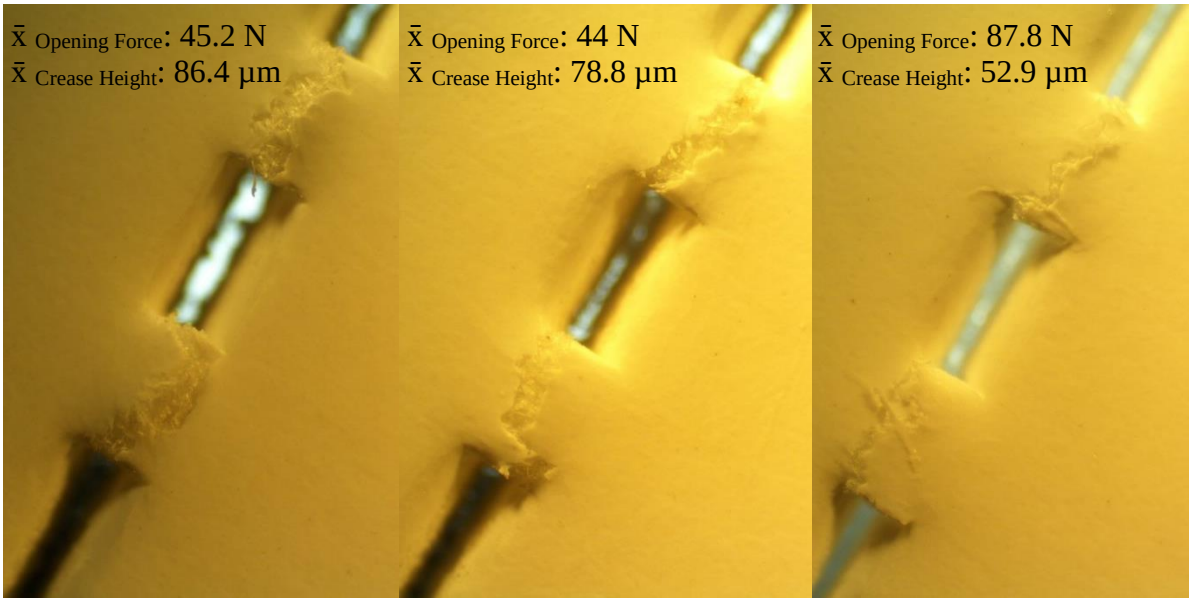

Figure 33. Perforation of paperboard A observed from the outside or paperboard side, A1 being the left image, A2 being the middle and A3 the right image.

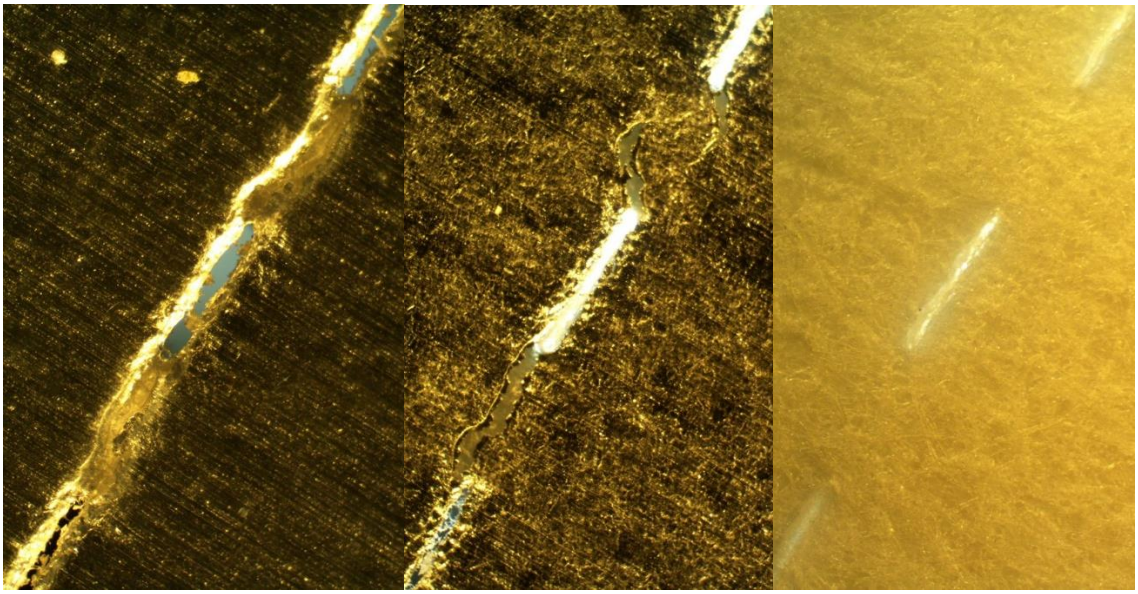

Figure 34. Perforation of paperboard A observed from the inside or laminate side, A1 being the left image, A2 the middle and A3 the right image.

Figure 35 and Figure 36 shows the perforation of paperboard B, being the most durable paperboard of the three in this study. Evidently, the laminate held together better. Laminate B1 has a total rupture in the outermost layer of the paperboard and a total rupture in the aluminum foil, while B2 has a partial rupture in the paperboard and aluminum foil and B3 is completely intact.

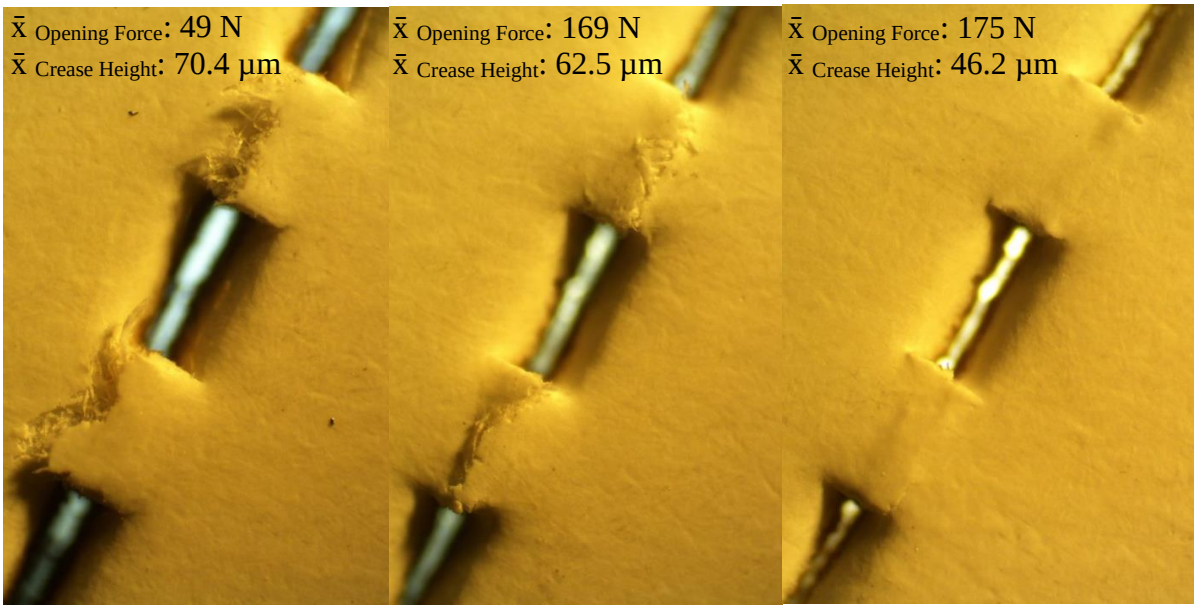

Figure 35. Perforation of paperboard B observed from the outside or paperboard side, B1 being the left image, B2 being the middle and B3 the right image.

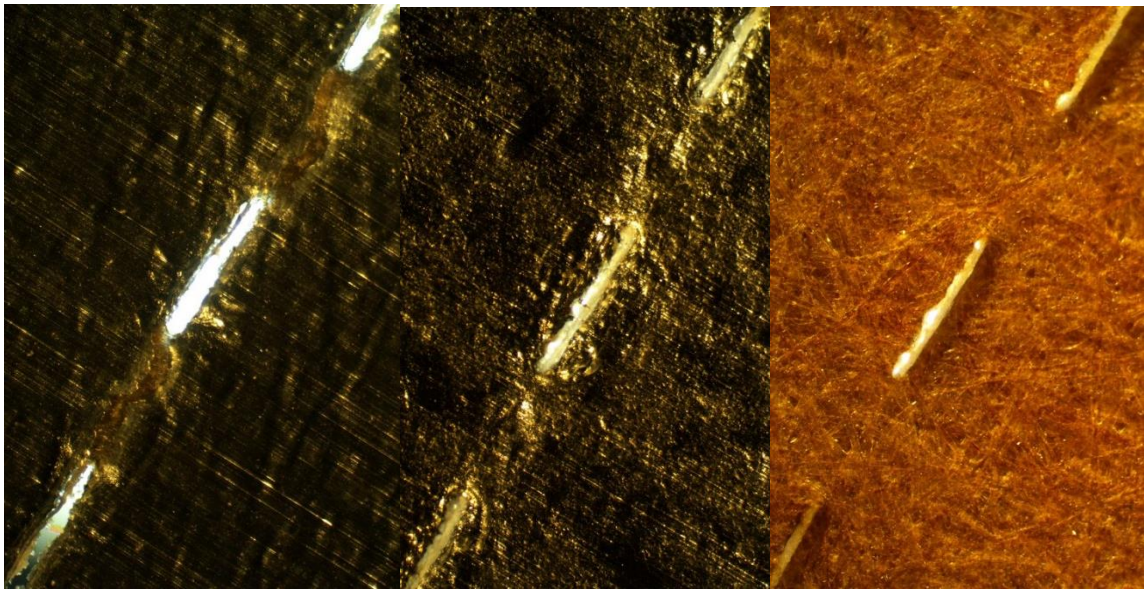

Figure 36. Perforation of paperboard B observed from the inside or laminate side, B1 being the left image, B2 the middle and B3 the right image.

Figure 37 and Figure 38 shows the perforation of paperboard C, being the weakest paperboard of the three in this study. All three laminates C1, C2 and C3 are completely ruptured in the outermost paperboard layer, as well as the aluminum foil in C1 and C2 being torn apart.

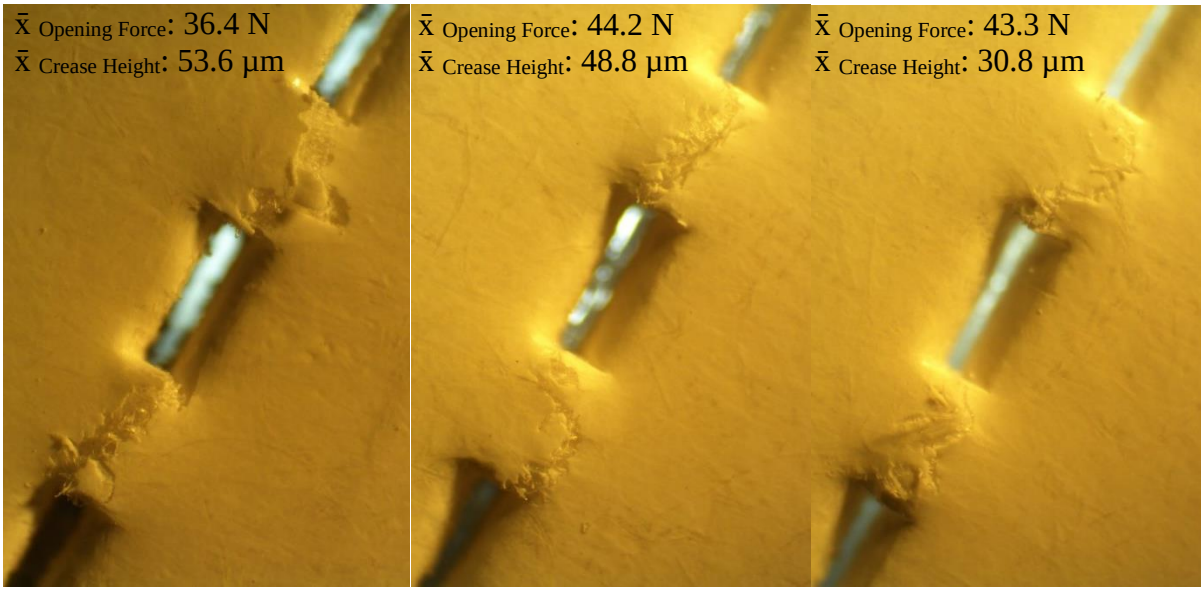

Figure 37. Perforation of paperboard C observed from the outside or paperboard side, C1 being the left image, C2 the middle and C3 the right image.

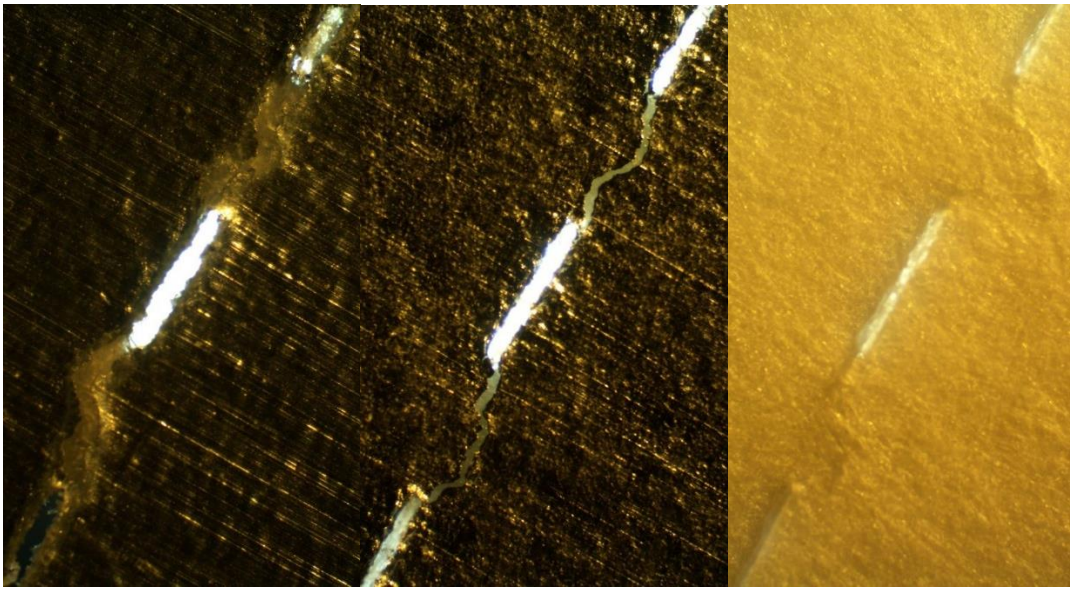

Figure 38. Perforation of paperboard C observed from the inside or laminate side, C1 being the left image, C2 the middle and C3 the right image.

5.6.2 High Resolution X-Ray microscopy & Computed Tomography

In total, five laminates were inspected in the high-resolution x-ray microscope. The five laminates inspected were A1, B3, C2, C3 produced in the flatbed die-cutter and one sample of A1 produced in the rotary die-cutter.

In Figure 39, a close up of the rupture in one of the perforation nicks of laminate A1 can be seen. The laminate was die-cut in the flatbed die-cutter. The thickest layer with the distorted appearance is the paperboard, with the clay layer on the uppermost part of the image. The thin bright layer under the paperboard is the aluminum foil, followed by a thicker PE-film at the bottom of the image. It is evident that the aluminum foil together with the paperboard are ruptured, and the only thing being intact is the polyethylene film closest to the bottom of the figure.

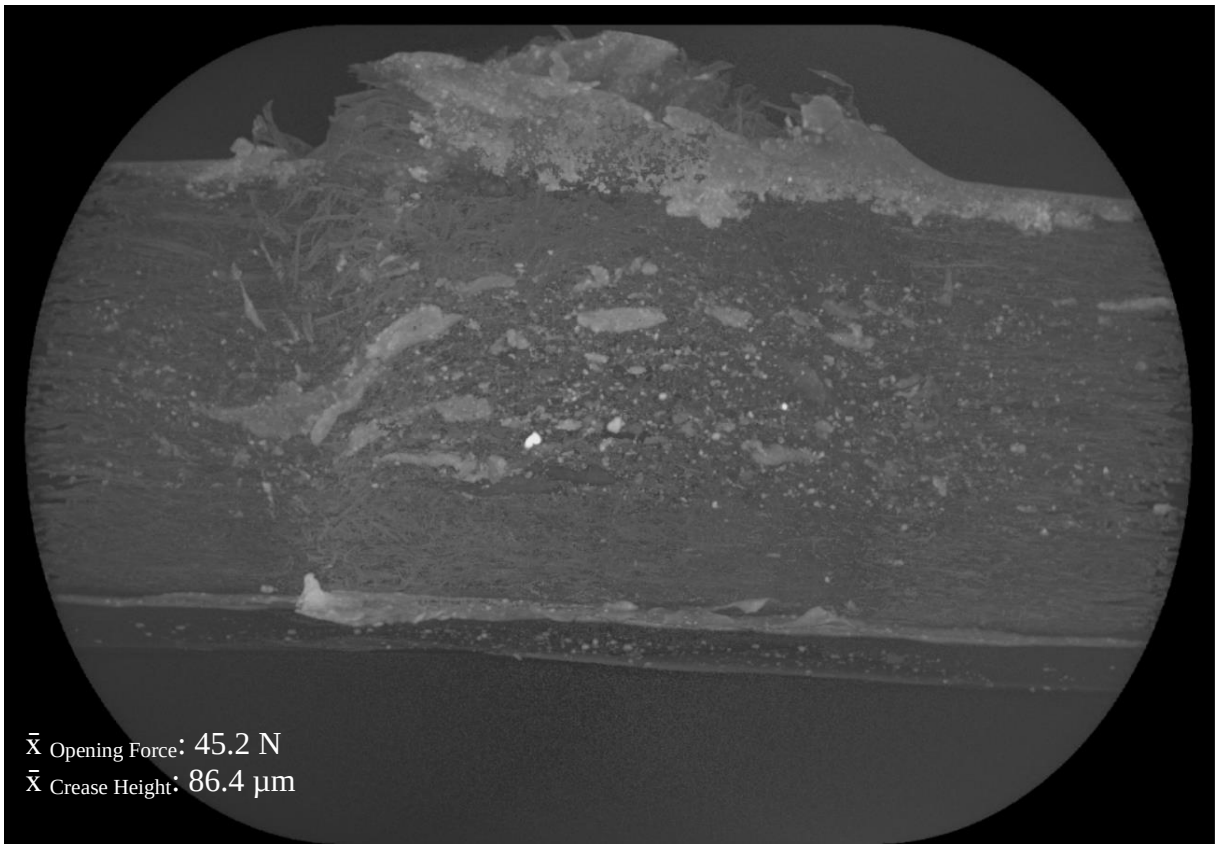

Figure 39. The rupture in a perforation nick of laminate A1, produced in a flatbed die-cutter. The paperboard and aluminum foil are ruptured.

Figure 40 shows the same laminate A1, but instead die-cut in a rotary die-cutting machine. The appearance is somewhat the same to the flatbed die-cut laminate, except for that the clay layer is somewhat less distorted than in Figure 39. Both the paperboard and the aluminum foil are ruptured in Figure 40.

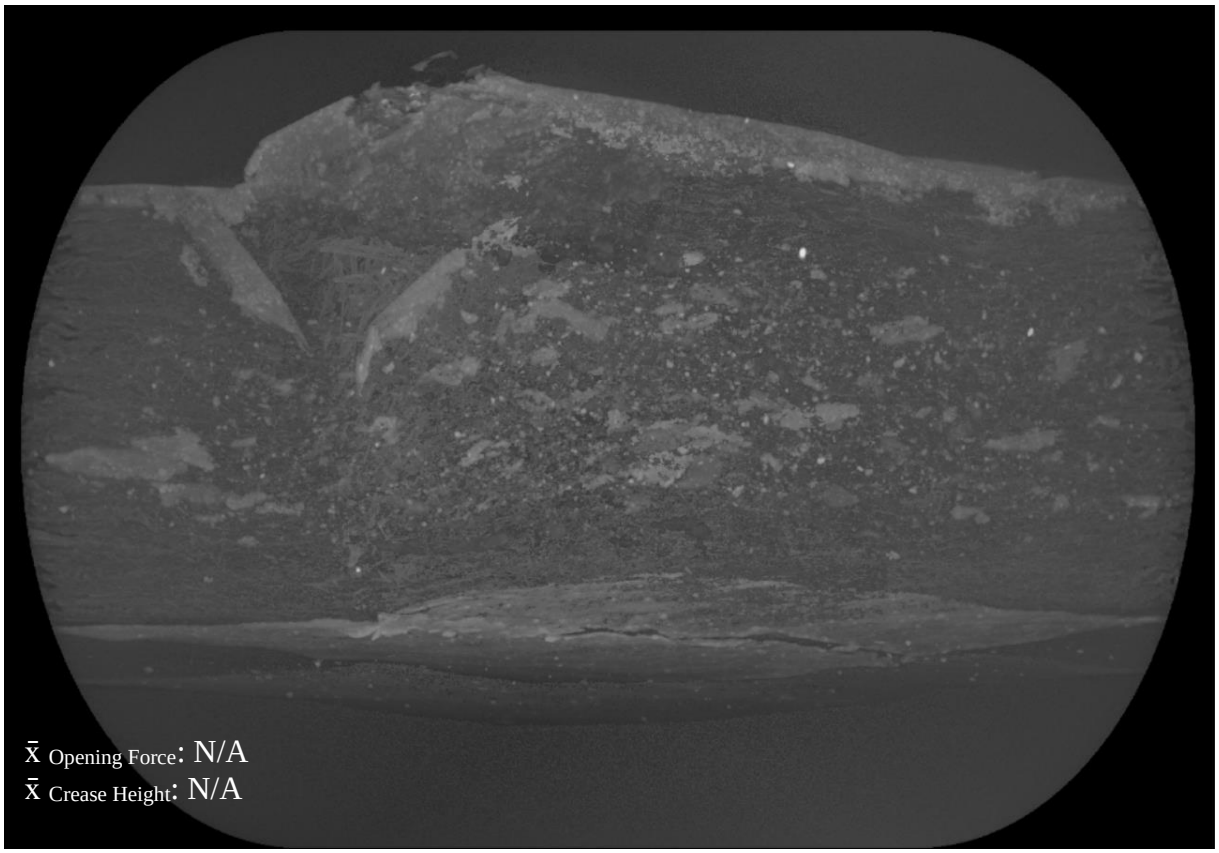

Figure 40. The rupture in a perforation nick of laminate A1, produced in a rotary die-cutter. The paperboard and aluminum foil are ruptured.

In Figure 41, an image laminate B3 die-cut in the flatbed die-cutter can be seen. Note that B3 does not have either the aluminum foil or the PE-film, just a thin layer of extrusion laminated PE barely visible in the bottom of the image. The rupture in the perforation does not pass through the entire perforation, as the layers of fibers closest to the PE-film are still intact. Regarding the clay layer in laminate B3, there is no clear rupture, and this is also confirmed by the right image in Figure 35.

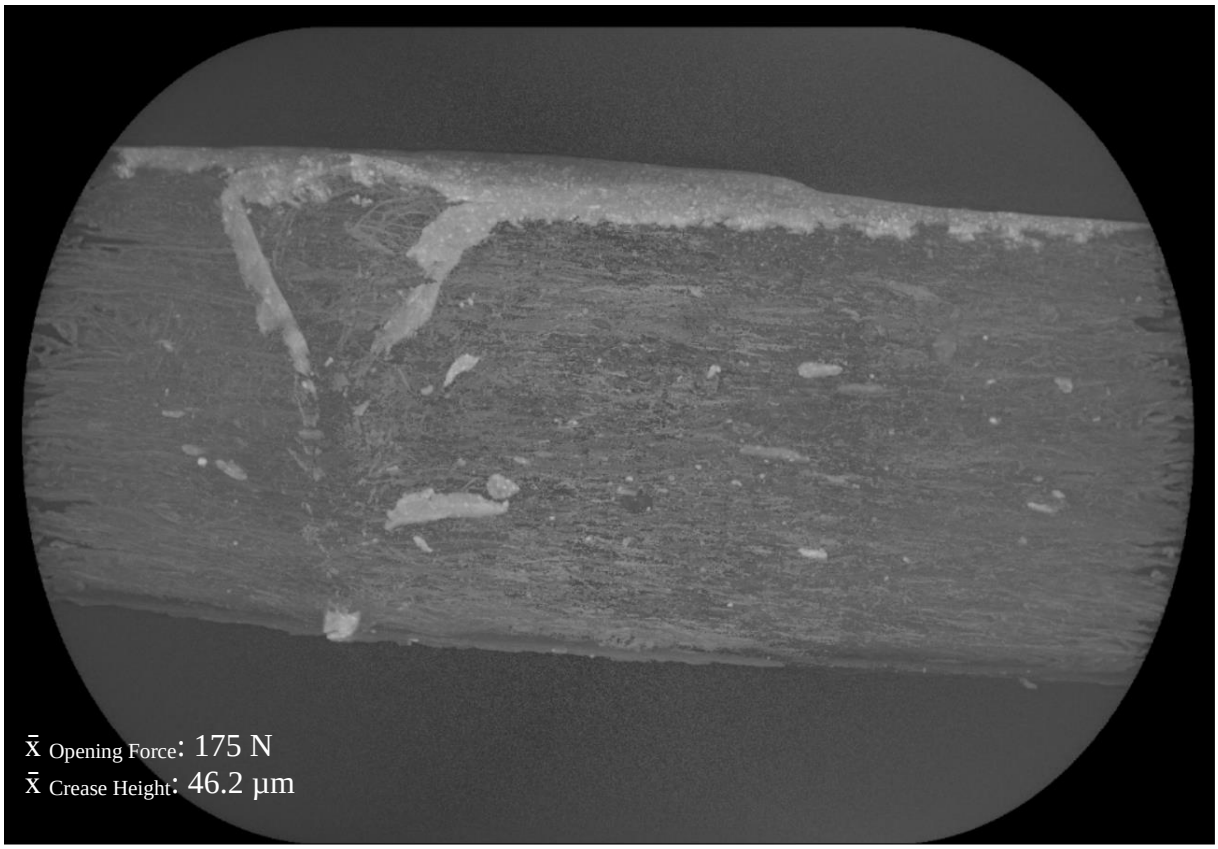

Figure 41. The rupture in a perforation of laminate B3, produced in a flatbed die-cutter. The paperboard is ruptured.

In Figure 42, an image of laminate C2 die-cut in the flatbed die-cutter can be seen. Laminate C2 does not have any PE-film but has the aluminum foil integrated in the laminate. Paperboard C is the paperboard with weakest mechanical properties of the three paperboards examined, which is noticable when studying Figure 42. As can be seen, the rupture in the laminate is wide and deep, penetrating the entire paperboard layer and the aluminum foil.

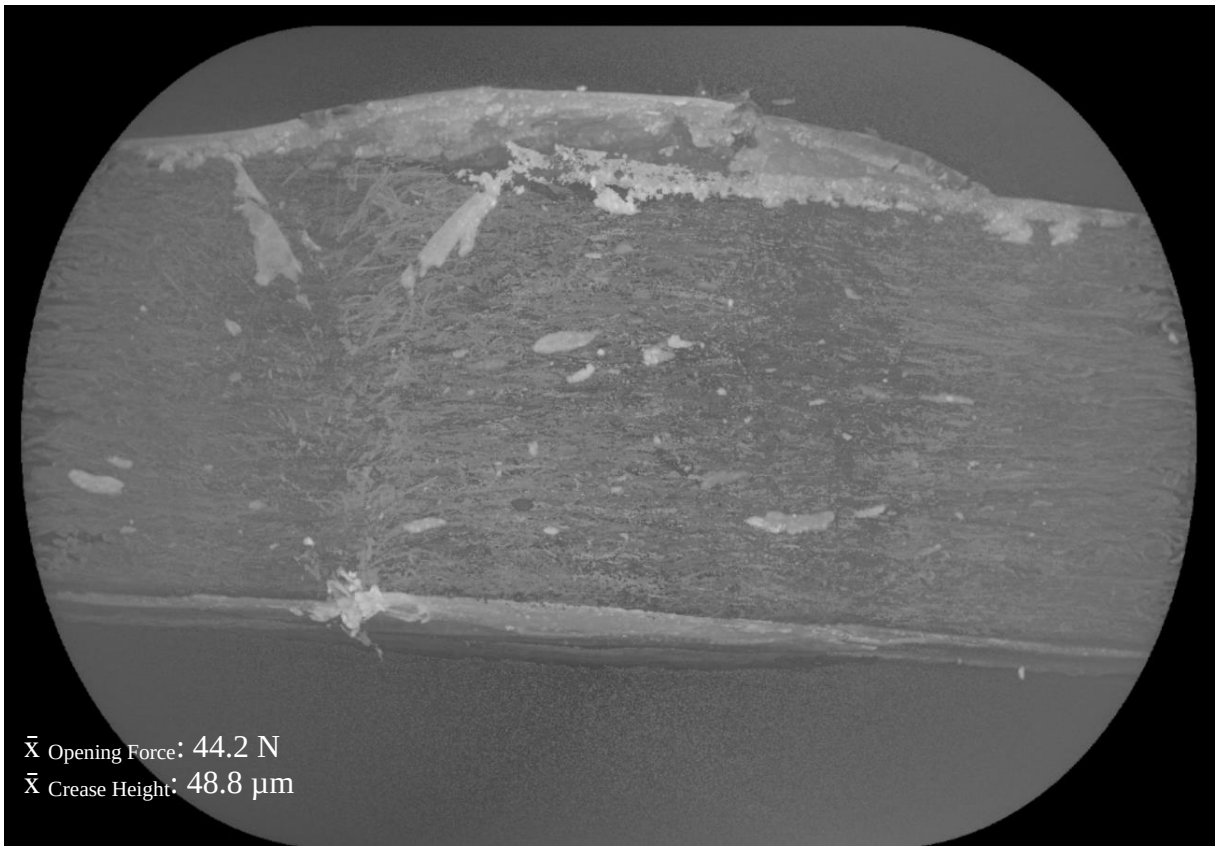

Figure 42. The rupture in a perforation of laminate C2, produced in a flatbed die-cutter. The paperboard is ruptured.

In Figure 43, the rupture of a perforation in the last laminate being C3 can be seen. Just as B3, this laminate has no PE-film or aluminum foil. The rupture penetrates the entire paperboard down to the thin PE layer. The top bleached paperboard layer is heavily distorted, and the fibers are visibly damaged in the perforation.

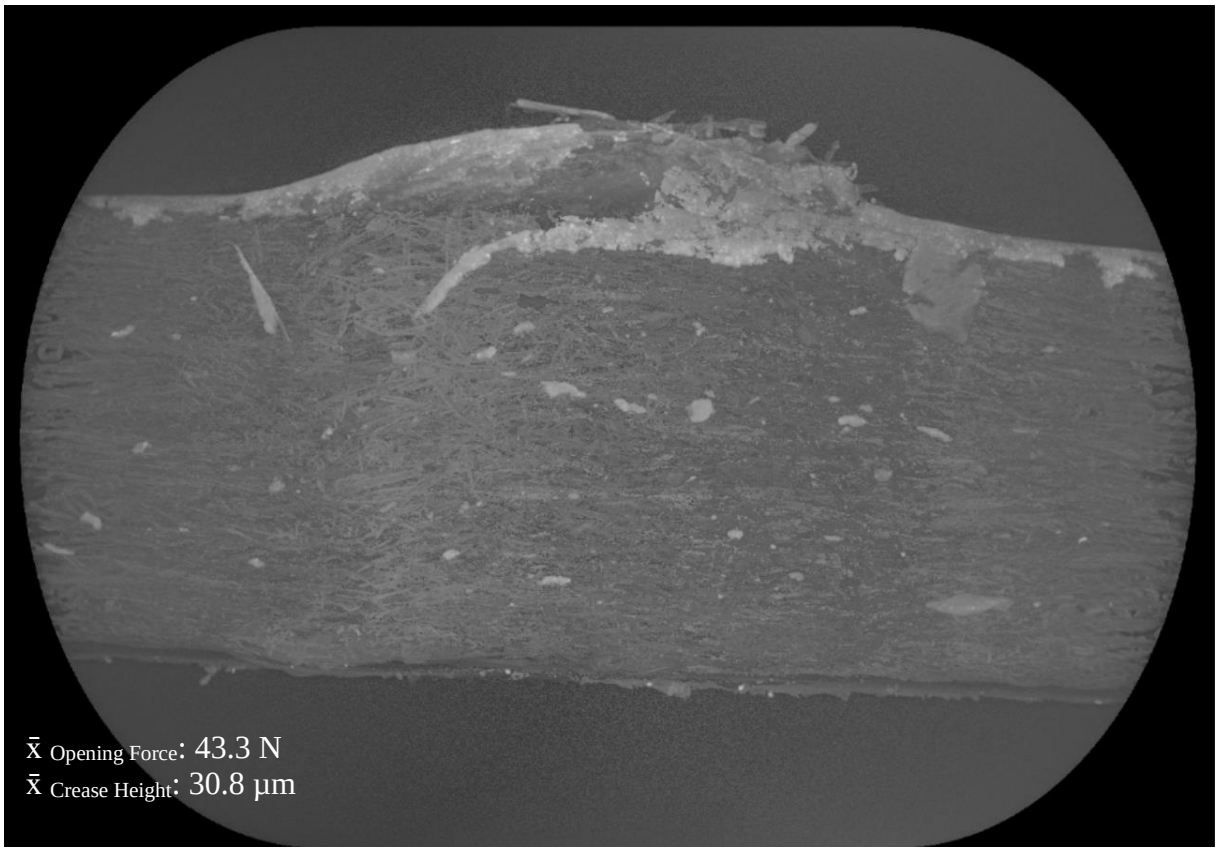

Figure 43. The rupture in a perforation of laminate C3, produced in a flatbed die-cutter. The paperboard is ruptured.

6 Discussion

When comparing the results for opening forces for the different laminates, it becomes evident that laminates with paperboard A performs best. This should come as no surprise since the die-cutting machine was set in accordance to laminate A1. Laminate A2 is also within an acceptable range for opening, while A3 is clearly over the acceptable range. It can also be noted that the mean standard deviation within each position is significantly greater in both A2 and A3 than in A1. For laminate B2 and B3, the measurements were discontinued since the opening strength exceeded the limitations of the tensile testing machine. In order to acquire any data with regards to B2 and B3, two samples from each laminate were tested in another stronger tensile testing machine, where opening forces way over the desired target force were noted, as can be seen in Table 6. Due to the time-consuming sample preparation for measurements of opening force in the stronger tensile testing machine together with the fact that the initial measurements were way past the desired opening force and not comparable with the opening forces of the other laminates, it was decided to halt the testing and prioritize further studies, such as qualitative analysis of the laminates.

Regardless of the lack of data for laminates with paperboard B, there is still an apparent tendency to be observed in laminates of paperboard A and C: more components in the laminate i.e., PE-film and aluminum foil, creates a die-cut laminate with lower perforation strength. At first, this was a somewhat bewildered finding, since a thicker laminate with more components theoretically would yield in a stronger perforation. Further qualitative investigations in an optic microscope revealed a possible explanation to the correlation between thinner laminates and stronger perforation strengths. As can be seen in Figure 33, Figure 35 and Figure 37, the degree of rupture in the paperboard is largest in the full laminate being A1, B1 and C1. Thereafter, a partial rupture can be observed in laminate A2, B2 and C2. Finally, Laminate A3, B3 and C3 can be observed with only a minimal visible rupture in the perforation. Since the paperboard contributes to a significant majority of the mechanical properties of the laminate, the degree of rupture in the paperboard strictly dictates the perforation strength. Therefore, laminates A1, B1 and C1 are the laminates with the weakest opening strength due to the largest degree of rupture in the paperboard, even though the laminates are the thickest and contain both PE-film and aluminum foil. A similar correlation can be seen from the inside of the laminates, see Figure 34, Figure 36 and Figure 38. The aluminum foil can clearly be seen only partially ruptured in laminate A2, B2 and C2, meanwhile the aluminum foil in A1, B1 and C1 is observed to be totally ruptured.

The possible explanation of why thicker laminates are weaker in opening force was strongly confirmed when analyzing the findings from the measurements in the x-ray microscopy. Laminate A1, C2 and C3 all have an entirely ruptured paperboard in the perforation, as can be seen in Figure 39, Figure 42 and Figure 43. This implies that the only contributor to the opening force in these laminates are other components than paperboard, such as the PE-film, which is elastic and therefore not ruptured by the force of the die in the die-cutting process. Regarding laminate B3 which can be seen in Figure 41, the paperboard is not entirely rup-

tured, consequently yielding in an exceptionally higher opening force, seen in Table 6. To yield a lower opening force, more suitable for consumer packaging applications, the partial rupture needs to be deeper, penetrating more fibers closer to the PE. Finally, this implies that there is a significant importance of including PE-film in the laminates that are die-cut with perforations, as this significantly simplifies the ability to control the opening force of the perforations and leads to easier setups and better production efficiency. When die-cutting laminates without PE-film such as B3, the opening force is strictly governed by the degree of partial paperboard rupture, which is significantly harder to control when producing large volumes of perforated die-cut laminates.

When studying the overall crease height, a general trend could be observed in which thicker laminates also had bigger crease height. In the opening force measurements, it was observed that the opening force increased for all paperboards from laminate 1 to laminate 3. However, in the case of crease height the opposite was observed, i.e., the crease height instead decreased for all paperboards from laminate 1 to laminate 3 as can be observed in Figure 18, Figure 19 and Figure 20. This pattern was expected since thicker laminates in general contain "more material" and thus there is more material to crease ultimately resulting in a bigger decrease in material thickness once it has been die-cut. In terms of best crease height, laminate A1 was observed to be the one performing the best, as can be seen in Table 10, this further implies that laminate A1 will be the easiest material to work with in the folding process since the bending resistance of the laminate has been reduced significantly. Although this should not come as a surprise since the flatbed die-cutters were originally tuned after laminate A1 and kept constant during all trial-runs with all different laminates.

However, with the reasoning mentioned above regarding the relationship between the crease height and the laminate thickness. One should expect laminates of paperboard B to have the biggest crease height since those laminates are the thickest, according to Table 10. Comparison between Table 10 reveals that it is not the case. One possible explanation to this deviation is that the paperboard B performs better in terms of mechanical properties. As mentioned above in section 4.4.2, paperboard B has a higher tearing strength, bending resistance, bending stiffness as well as tensile- and burst strength than paperboard A and C. Another possible explanation is once again the fact that the flatbed die-cutter was tuned according to paperboard A, more specifically laminate A1, and therefore led to the crease height of paperboard B becoming lower although it is thicker.

Lastly, regarding the possible correlation between crease height and material thickness, another element that influences the crease height is how the material fits the crease channels (where the creases are formed in the punch plate). Using the same dimensions of the crease channels as has been done in this thesis, a thicker laminate (i.e., laminate A01) will fill the crease channel and cause the laminate in close proximity to the crease to experience high stress loads. Since the nicks are near the creases, this intends that the nicks experience a high stress load and therefore tend to rupture, which can be seen in the images acquired both from the optic microscope and the high-resolution 3D x-ray microscope. If the laminate in mind instead is thin (i.e., laminate A03), the laminate will not fully fill the crease channel and instead be able to loosely fit into the channel, resulting in a potentially lower stress near the creases due to the looser fit of the laminate in the crease channel. Therefore, the nicks in laminates with a thinner structure are not as affected by the top creasing, and result in a lower

degree of rupture, as can be seen in the images acquired both from the optic microscope and the high-resolution 3D x-ray microscope.

The paired tests of opening force and crease height conducted solely on the laminates of paperboard A showed that there is a negative relationship between the crease height and opening force. Meaning that lower crease height resulted in higher opening forces. Although this seems to be the case for the results in Figure 21 and Table 11 in section 5.3, one should not jump to that conclusion all too fast. Based on the reasoning above, it has been observed that thicker material implies a thicker crease height. While at the same time, thicker material has laminates that consists of more material which in turn has been shown to have ruptured perforations, yielding in a lower opening force as mentioned earlier, also illustrated by Figure 33, Figure 35 and Figure 37. Therefore, it is not possible neither completely true to conclude that the crease height is the only factor that affects the opening force in this way. In addition, this possible correlation was only studied for laminates of paperboard A which further indicates the weakness of the proposed correlation.

Considering the additional opening force measurements of samples produced with the digital die less cutting and creasing table, it is noted that the trend in opening force opposes the trend of laminates produced in the flatbed die-cutter. The samples produced with the cutting table show a clear and significant trend that when adding more layers, the laminate is reinforced and yields in a higher opening force, regardless of what paperboard is showcased. For the flatbed die-cut samples, an exact opposite tendency is observed, that when adding more components, the opening force is weakened. This further strengthens the theory that during addition of components (such as al-foil and the PE-film) to the laminate, the integrity of the entire perforation line is affected when die-cut, as the fibers in the paperboard are torn and destroyed, drastically decreasing the opening force.

The results from the trial runs in the rotary die-cutter shows the same tendency in opening force as the results obtained from the flatbed die-cutter. Namely that the opening force increases as the number of components in the laminate decreases. Which further confirms the pattern that more components in the laminate results in weaker perforations and thus weaker opening force.

In the qualitative results it was observed that in laminate 1 of all paperboards the paperboard was completely ruptured in every case. The rupture went all the way from the top ply of the paperboard, through the al-foil and up until the PE-film. In the X-ray microscopy, see section 5.6.2, it was observed that it is only the PE-film that is holding the material together, everything else is and/or has been destroyed. This phenomenon could also further explain why materials with laminate 1 had less spread in data and a lower standard deviation than materials with laminate 2 or 3. Since the PE-film is a homogenous material, it will “behave” in a similar way in almost all cases, thus resulting in opening forces with less spread. When on the laminates 2 were examined using 3D X-ray tomography it was noted that rupture once again went all the way through up until the al-foil. For laminate 2 the same reasoning still follows, meaning that al-foil is a more homogenous material and thus it will behave in a similar way in

many of the cases, which is further illustrated by looking at the standard deviations for paperboards with laminate 2. Lastly, tomographic examination of laminate 3 shows that laminates are not always ruptured all the way through the paperboard. Since paperboard is not a homogenous material this implies that its body blanks will not behave in a similar way all the time as the opening force now is more dependent upon the degree of rupture within the paperboard layer of the laminate.

Although the initial opening force measurements showed some surprising results, namely the pattern in which the opening force increased as the total material thickness (and the number of components in the laminate) decreased. However, up until this point the processing method of the paperboard has not been taken into great account. Paperboard B is the paperboard that has been shown to be the absolute toughest, this has to do with the fact that several of plies of its multi-ply structure constitutes of unbleached chemical pulp. In the theory it was mentioned that chemically pulped fibers results in fibers that are longer, furthermore this implies that the fibers in the fiber network are intertwined much better. On top of that, the absence of bleaching agent proceeding the pulping results in the fiber network keeping its integrity which in the end yields a product with significantly higher mechanical properties. Even though the transition into a completely fiber-based solution puts more demands on the mechanical properties of the paperboard due to the lack of hard-plastic components, the answer does not seem to lie in using paperboards with all too high mechanical properties. When investigating Paperboard A, it seems most suitable for the Boardio application according to this study. According to theory, the paperboard should be the one to perform best for folding and converting processes. However, one should also bear in mind that one of the constraints in this thesis was that no change in machine setup was made and that the die-cutter was set after laminate A1, hence this could also contribute to the better performance of the paperboard.

7 Conclusions

This section aims to summarize and conclude this report, concisely presenting the findings of the different measurements and inquiries done within the scope of this thesis. A more comprehensive dialogue can be found under section Discussion.

In general, the following conclusions can be drawn.

- When die-cutting in the flatbed die-cutter, it is less difficult to sequential produce creases first, followed by perforations in the next operation and keep a good quality of both the creases and perforations, due to the challenge of handling the induced stresses in the laminate in close proximity to the creases when forming perforations and creases simultaneously. However, this is not desired due to the higher run-time and waste.
- When die-cutting (flatbed & rotary) perforations in laminates for the Boardio® system, laminates with PE-film generally yield in easier process control and opening forces with lower spread, as the only component contributing to the opening force is the PE-film due to the complete rupture of the paperboard.
- When tuning the opening force in laminates for the Boardio® system that do not have a PE-film, the opening force is instead strictly governed by the partial rupture of the paperboard in the perforations.
- The crease height depends on the thickness of the laminates for the Boardio® system, as thicker laminates yield in significantly larger crease height. However, this is not entirely true, as paperboards with high mechanical strength tend to be more difficult to crease.
- Thicker laminates tend to have a larger degree of rupture in the nicks of the perforation than thinner laminates. This can be explained by the higher induced stresses in close proximity to the creases of thicker laminates, as the laminate fills the crease channels, when compared to thinner laminates which sit more loosely in the crease channels and therefore induce a lower stress in close proximity to the creases.
- Perforations produced with a cutting table yield in opening forces that are higher for laminates with more components and higher thickness i.e., PE-film and aluminum foil. This is the opposite of laminates produced in both the flatbed die-cutter and rotary die-cutter, as they decrease in opening force as they become thicker (due to the increasing degree of rupture in the paperboard). In addition, this behavior has its explanation in the fact that the cutting table only perforates and does not crease the samples thus leading to no ruptures of the “plotted” samples.
- The results of the opening force measurements indicate that some paperboards may fit better for the Boardio application than others. Paperboard B with high mechanical strength due to the unbleached chemical pulp layers proves to be difficult to convert/process.

7.1 Future Work

- Conduct a similar study to this, with the goal to yield in the same opening force and crease thickness for the different laminates, by tuning the die-cutter machine settings depending on the material instead of keeping the settings constant as in this study.
- Conduct a trial run in the die-cutter where the aim is to investigate if there is a correlation between opening force of the body blanks and order of production (i.e., position in a pallet). Suggested approach: tune the die-cutter after A01 so that the opening force and crease height is within the favorable limits. Do this with as few sheets as possible and note the number of sheets used for the setup. Thereafter, take out ten samples followed of die-cutting of 50 sheets and take out ten samples again of each position. Repeat the procedure for 1000 sheets. This should yield in 16 different measurement points/1000 sheets with ten samples/measurement point, a total of 1280 body blanks (if run on 8 body blanks/sheet). Measure the opening force of the body blanks and note the measurement point (i.e., position in the produced pallet) and present the data as a function of sample number. Each position should have 160 data points, where the first data point is the first sample, and so on.
- Investigate if there is a correlation of the opening force of body blanks and finished Boardio container. Suggested approach: tune the die-cutter after A01 so that the opening force and crease height is within the favorable limits. Produce at least one pallet of die-cut body blanks before taking any samples for measurement. From approximately the same position of the pallet, take 40 samples of each position and measure 20 of the samples immediately. For the remaining 20 samples/position, construct Boardio containers and test the opening force of the containers. Compare and evaluate if there is a significant difference in opening force between body blanks and Boardio containers.
- Test “pure” paperboard, i.e., paperboard that has not been laminated, as this was not possible since it risked ruining die-cutting forms.
- Further qualitative evaluations with high-resolution x-ray microscopy to fully understand the practical implications of die-cutting paperboard laminates and how this affects the mechanical properties and attributes of die-cut material (such as the creasing and perforation).
- Investigate the possibility of establishing a FEA/FEM simulation of the creasing and cutting/perforating of laminates to deeper understand the process, as well as making better predictions in process and material pairing for possible future paperboard and laminate structures.
- Test different perforation configurations in the flatbed die-cutter with the same nine laminates as investigated in this thesis. Suggested approach: construct a test-die with several configurations to test larger volumes of material in less time.

8 References

[1] AR-Packaging. (2022). *Our story*. Available: https://www.ar-packaging.com/en/our-business/our-story

[2] J. Fowle and M. J. Kirwan, "Paper-based flexible packaging," in *Handbook of Paper and Paperboard Packaging Technology*, 2013, pp. 91-123.

[3] Y. Ottosson, "Quality improvement of sheeted materials," Project report, 2021.

[4] S. Nagasawa, Y. Fukuzawa, T. Yamaguchi, S. Tsukatani, and I. Katayama, "Effect of crease depth and crease deviation on folding deformation characteristics of coated paperboard," *Journal of Materials Processing Technology - J MATER PROCESS TECHNOL*, vol. 140, pp. 157-162, 09/01 2003.

[5] M. J. Kirwan, M. J. Kirwan, Ed. *Handbook of paper and paperboard packaging technology*, 2nd ed ed. Chichester, West Sussex ; Ames, Iowa: Wiley-Blackwell, 2013.

[6] M. Nygårds, M. Just, and J. Tryding, "Experimental and numerical studies of creasing of paperboard," *International Journal of Solids and Structures*, vol. 46, no. 11, pp. 2493-2505, 2009/06/01/ 2009.

[7] M. Hallin, "Personal Communication," Y. Qasem and Y. Ottosson Chraibi, Eds., ed: Graphic Packaging International Systems, 2022.

[8] A. Riley, "10 - Paper and paperboard packaging," in *Packaging Technology*, A. Emblem and H. Emblem, Eds.: Woodhead Publishing, 2012, pp. 178-239.

[9] B. Davidsdottir, "Forest Products and Energy☆," in *Reference Module in Earth Systems and Environmental Sciences*: Elsevier, 2013.

[10] P. J. Fellows, "24 - Packaging," in *Food Processing Technology (Fourth Edition)*, P. J. Fellows, Ed.: Woodhead Publishing, 2017, pp. 949-1044.

[11] P. Bajpai, "Chapter 19 - Pulp Bleaching," in *Biermann's Handbook of Pulp and Paper (Third Edition)*, P. Bajpai, Ed.: Elsevier, 2018, pp. 465-491.

[12] HOLMEN. (2022, 03-23). *From pulp to paper at Holmen Paper, Braviken Paper mill*. Available: https://www.holmen.com/en/paper/insights/paper-academy/paper-production/from-pulp-to-paper/

[13] T. Fadiji, T. M. Berry, C. J. Coetzee, and U. L. Opara, "Mechanical design and performance testing of corrugated paperboard packaging for the postharvest handling of horticultural produce," *Biosystems Engineering*, vol. 171, pp. 220-244, 2018/07/01/ 2018.

[14] T. Fadiji, C. J. Coetzee, T. M. Berry, A. Ambaw, and U. L. Opara, "The efficacy of finite element analysis (FEA) as a design tool for food packaging: A review," *Biosystems Engineering*, vol. 174, pp. 20-40, 2018/10/01/ 2018.

[15] A. Hagman, "Investigations of in-plane properties of paperboard," KTH Royal Institute of Technology, 2013.

[16] P. Tanninen, S. Matthews, V. Leminen, and J. Varis, "Analysis of paperboard creasing properties with a novel device," *Procedia Manufacturing*, vol. 55, pp. 232-237, 2021/01/01/ 2021.

[17] M. E. Biancolini, "Evaluation of equivalent stiffness properties of corrugated board," *Composite Structures*, vol. 69, no. 3, pp. 322-328, 2005/07/01/ 2005.

[18] G. L. Robertson, *Food packaging: principles and practice*. 2013.

[19] L. A. A. Beex and R. H. J. Peerlings, "An experimental and computational study of laminated paperboard creasing and folding," *International Journal of Solids and Structures*, vol. 46, no. 24, pp. 4192-4207, 2009/12/01/ 2009.

[20] C. Barbier, P.-L. Larsson, and S. Östlund, "Numerical investigation of folding of coated papers," *Composite Structures*, vol. 67, no. 4, pp. 383-394, 2005/03/01/ 2005.
[21] M. Nygårds, N. Hallbäck, M. Just, and J. Tryding, "A finite element model for simulations of creasing and folding of paperboard," in *Abaqus users' conference*, 2005.
[22] A. Giampieri, U. Perego, and R. Borsari, "A constitutive model for the mechanical response of the folding of creased paperboard," *International Journal of Solids and Structures*, vol. 48, no. 16, pp. 2275-2287, 2011/08/01/ 2011.
[23] T. Garbowski, T. Gajewski, and J. K. Grabski, "Estimation of the Compressive Strength of Corrugated Cardboard Boxes with Various Perforations," vol. 14, no. 4, p. 1095, 2021.
[24] S. Carmignato, W. Dewulf, and R. Leach, Eds. *Industrial X-Ray Computed Tomography*. Cham: Springer International Publishing, 2018.

9 Appendix

9.1 Appendix. A – Layout of a Die-cut Sheet

Figure 44 showcases a typical layout of a die-cut laminated sheet along with the positions. Each and every number represents the position, and each and every position is an actual body blank that will be folded into a container. The machine direction is upwards, and the cross direction is to the right. The die-cutting operation die-cuts and perforates the sheet in CD which in turn means that the perforation pulls in the MD.

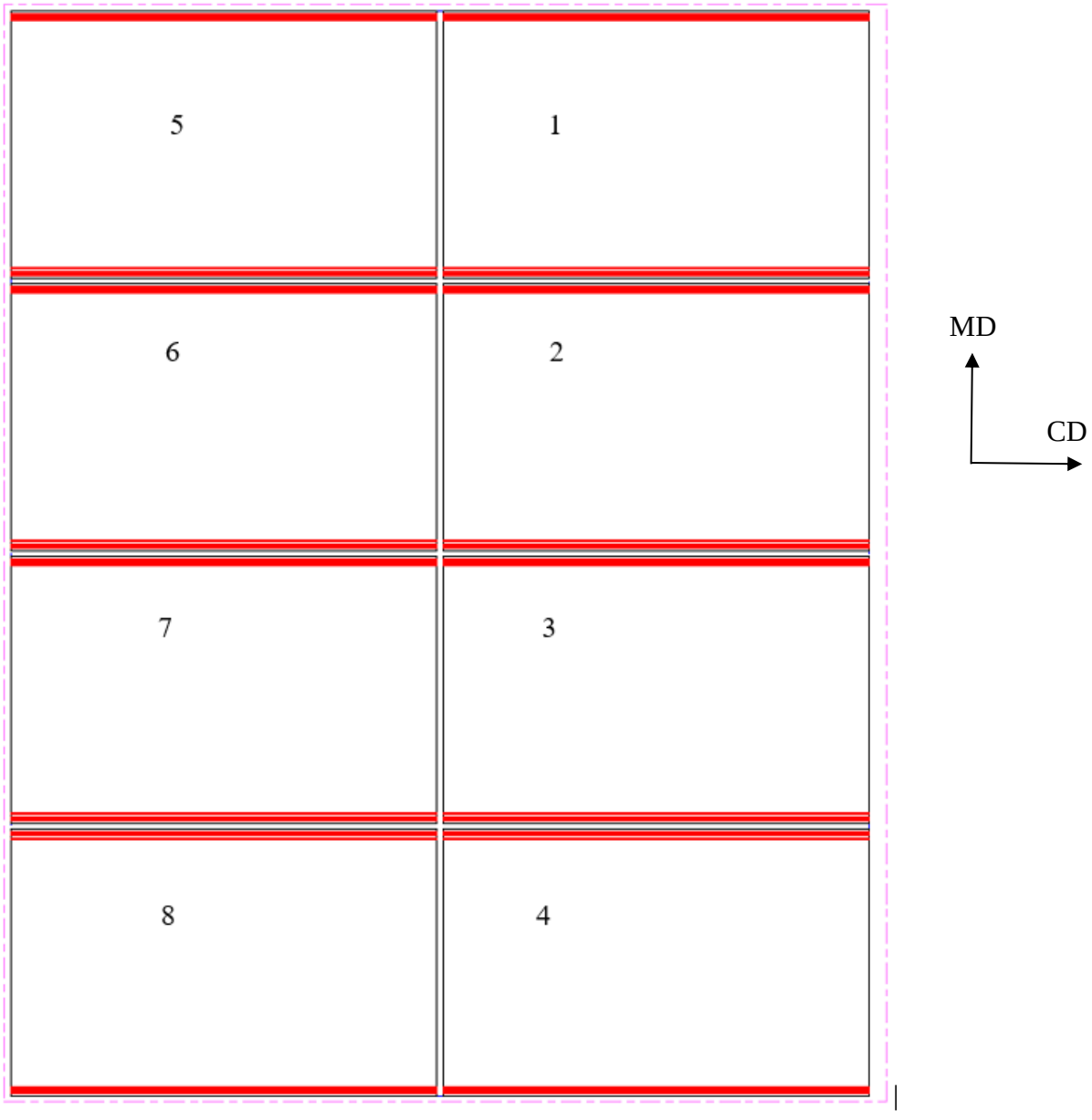

Figure 44. Illustrates how the body blanks are positioned on a die-cut laminate sheet.

9.2 Appendix. B – Top and Bottom Crease Thickness Measurements

9.2.1 Paperboard A

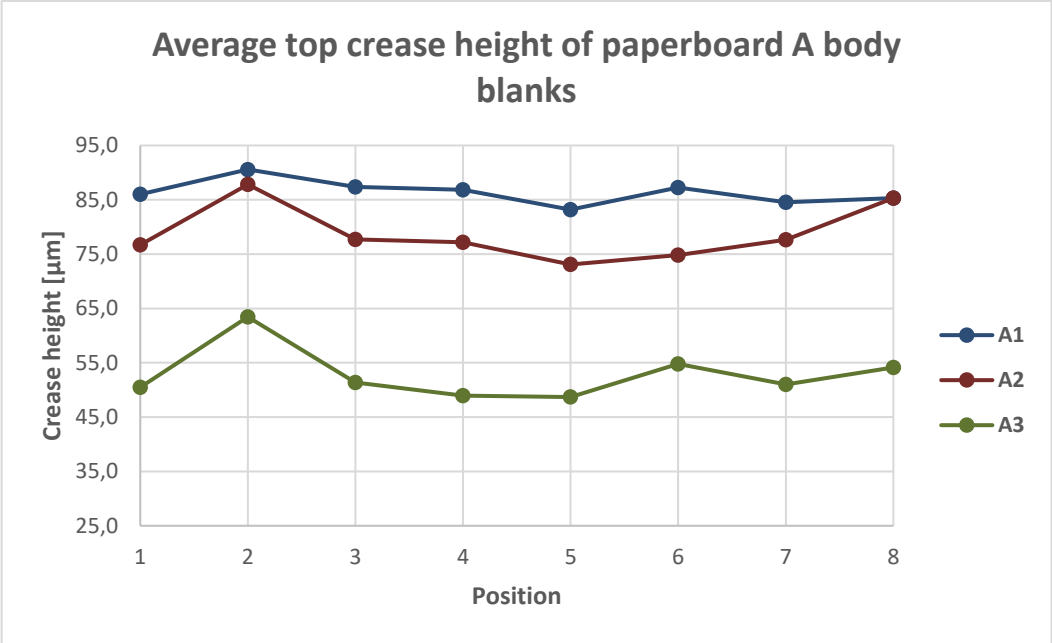

Figure 45. Illustrates how the average top crease height differs from position to position. The y-axis represents the crease height in µm, and the x-axis represents the positions 1-8.

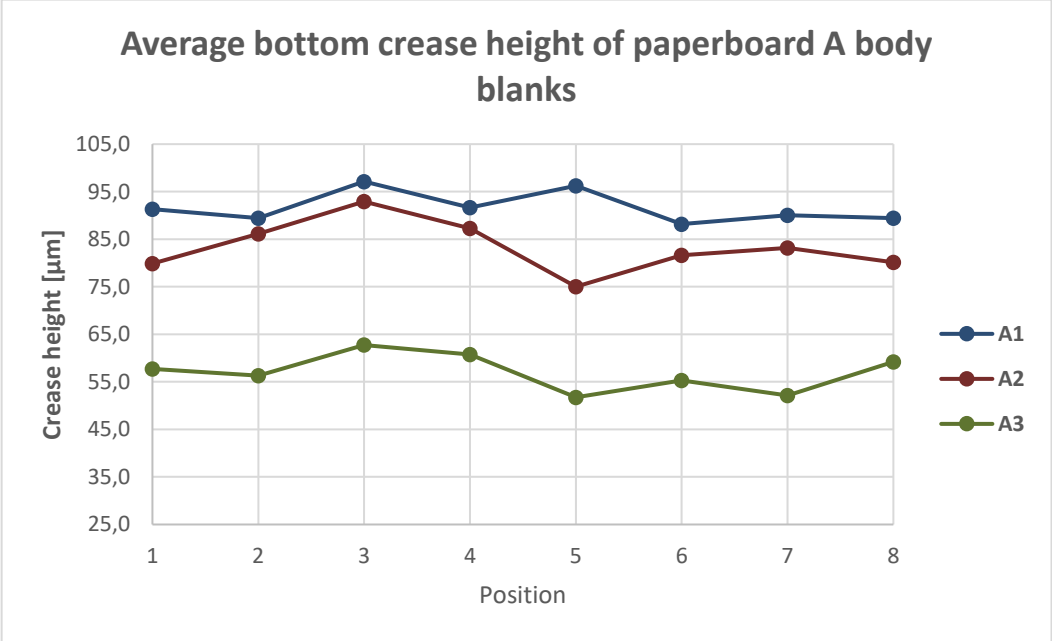

Figure 46. Illustrates how the average bottom crease height differs from position to position. The y-axis represents the crease height in µm, and the x-axis represents the positions 1-8.

9.2.2 Paperboard B

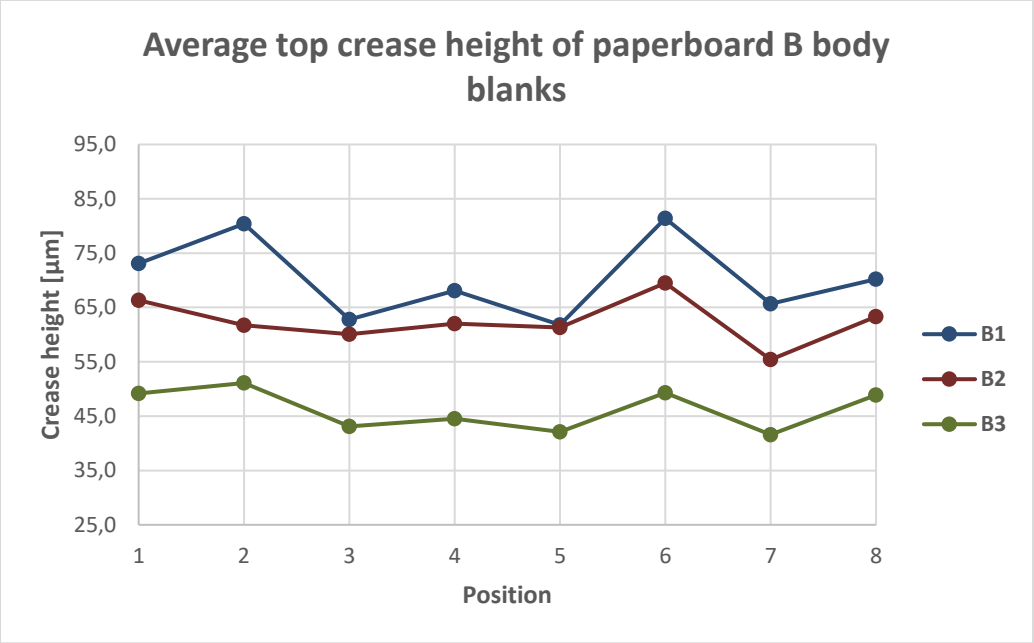

Figure 47. Illustrates how the average top crease height differs from position to position. The y-axis represents the crease height in µm, and the x-axis represents the positions 1-8.

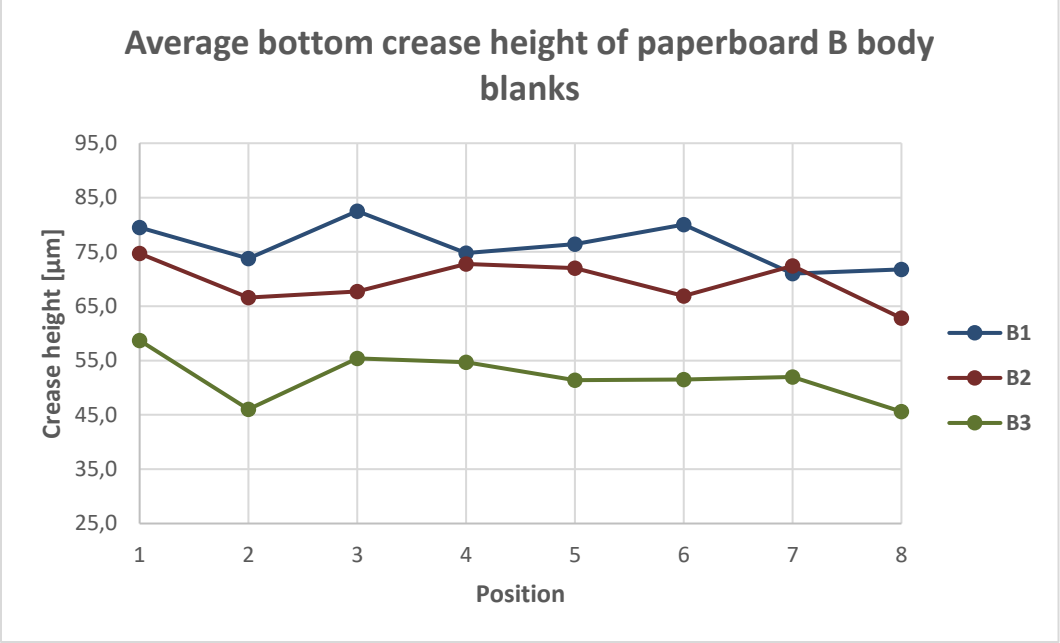

Figure 48. Illustrates how the average bottom crease height differs from position to position. The y-axis represents the crease height in µm, and the x-axis represents the positions 1-8.

9.2.3 Paperboard C

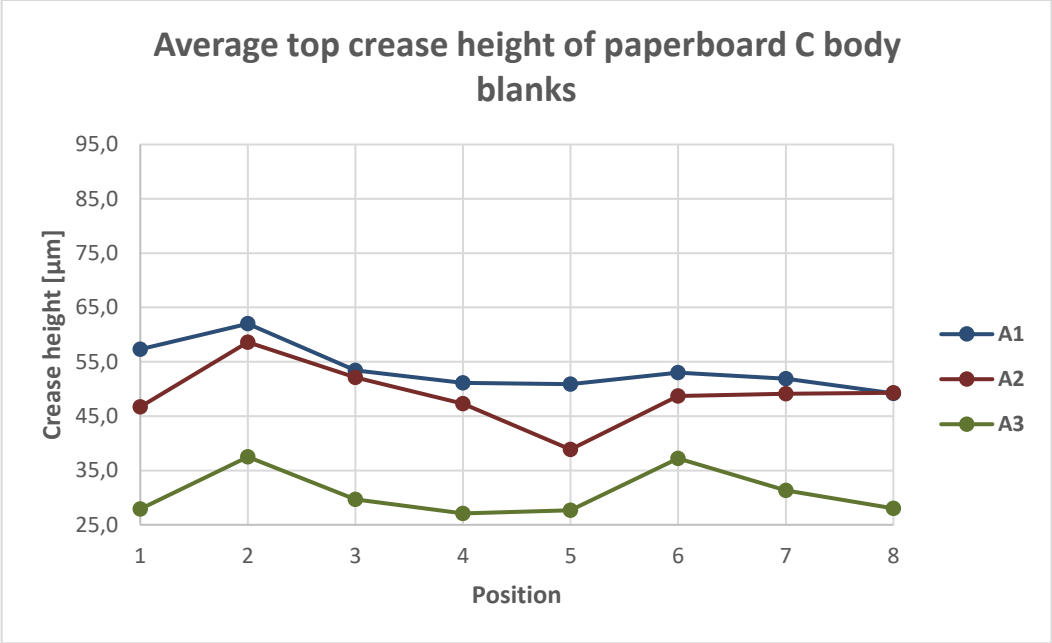

Figure 49. Illustrates how the average top crease height differs from position to position. The y-axis represents the crease height in µm, and the x-axis represents the positions 1-8.

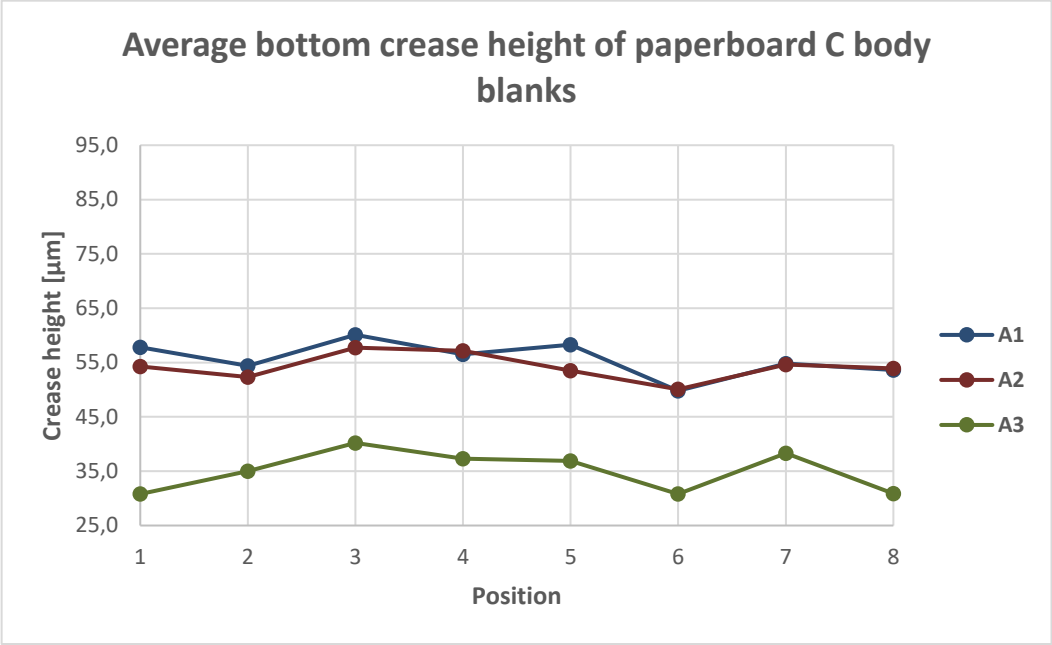

Figure 50. Illustrates how the average bottom crease height differs from position to position. The y-axis represents the crease height in µm, and the x-axis represents the positions 1-8.